Generating Asymmetric Einstein-Podolsky-Rosen Steering between Two movable Mirrors Exploiting Correlated-Emission Laser

Jamal El Qars[a,b], Ismail Essaoudi[a], and Abdelmajid Ainane[a,c]
[a] *Laboratory of Materials Physics and Systems Modelling, (LP2MS), Physics Department, Faculty of Sciences, Moulay Ismail University, Meknes, Morocco*
[b] *Laboratory of Materials, Electrical Systems, Energy and Environment, (LMS3E), Faculty of Applied Sciences, Ait-Melloul, Ibn Zohr University, Agadir, Morocco*
[c] *Max-Planck-Institut für Physik Complexer Systeme, Nöthnitzer Str. 38, Dresden 01187, Germany*

arXiv:2505.20449v1 [quant-ph] 26 May 2025

Abstract

Quantum steering is a form of quantum correlation that exhibits an inherent asymmetry, distinguishing it from entanglement and Bell nonlocality. It is now understood that quantum steering plays a pivotal role in asymmetric quantum information tasks. In this work, we propose a scheme to generate asymmetric steering between two mechanical modes by transferring quantum coherence from a correlated-emission laser. To accomplish this, we derive quantum Langevin equations to describe the optomechanical coupling between two cavity modes and two mechanical modes along with the master equation of two-mode laser. By examining the case where the cavity modes scatter at the anti-Stokes sidebands, we demonstrate that both two-way and one-way steering can be achieved by adjusting the strength of the field driving the gain medium of the laser. Furthermore, we show that the direction of one-way steering can be controlled by varying the temperatures of the mechanical baths or the strengths of the optomechanical couplings. Additionally, we reveal that the directionality of one-way steering depends on the modes fluctuation levels of the modes, with the mode exhibiting larger fluctuations determining the direction. This highly controllable scheme could potentially be realized with current technology, offering a promising platform for implementing one-way quantum information tasks.

1 Introduction

The quantum nonlocality of entangled states was first highlighted by Einstein, Podolsky, and Rosen (EPR) in 1935 [1], where they argued the incompatibility between local causality and the completeness of quantum mechanics. By examining a general nonfactorizable pure state of two particles, EPR demonstrated that a measurement performed on one particle seemingly induces an apparent nonlocal perturbation on the wave-function of other particle. For EPR, such nonlocal effects were unacceptable suggesting the need for local hidden variables. The EPR paper prompted a significant response later that year from Schrödinger [2, 3] who initially introduced the term *steering* to analyse the EPR paradox, and later extended the concept to mixed states. However, the formalization of quantum steering was only fully developed in 2007 [4].

In terms of the local hidden variable and local hidden state models, quantum steering was rigorously defined in [4] as a type of quantum correlation that allows an untrusted observer (e.g., Alice) to remotely influence the state of another trusted observer (e.g., Bob) through implementing local measurements [5]. Thus, steering is often described as a one-sided device-independent scenario for verifying of entanglement. In the hierarchy of nonseparable quantum correlations, steering is positioned between entanglement [6] and Bell nonlocality [7], being strictly stronger than the former, but strictly weaker than the later. In other words, not every entangled state displays steering, and not every steerable state demonstrates Bell nonlocality [8].

Unlike entanglement and Bell nonlocality, quantum steering is inherently asymmetric. A bipartite state shared between Alice and Bob may be steerable from Alice to Bob but not necessarily in the reverse direction, an asymmetry demonstrated both theoretically [9, 10, 11, 12, 13, 14] and experimentally [15, 16, 17, 18, 19]. This unique asymmetry has led to the recognition of EPR steering as a key ingredient for one-sided device-independent quantum key distribution (1SDI-QKD) [20], one-sided device-independent quantum secret sharing [21], universal one-way quantum computing [22], secure quantum teleportation [23], and subchannel discrimination [24]. For these applications, effective characterization of steerable states is essential, and considerable effort has been dedicated to developing criteria for determining whether a bipartite state is steerable [25, 26, 27] or for quantifying the degree of steerability in such states [24, 28, 29].

Observing quantum effects in macroscopic systems is of crucial importance, as it can deepen our understanding of quantum nonlocality. Cavity optomechanics, as an emerging field studying the strong coupling between optical and mechanical degrees of freedom via radiation pressure [30], offers a promising platform for exploring entanglement [31], squeezing [32], optical bistability [33], ground state optical feedback cooling of fundamental mechanical modes [34], and even Schrödinger's cat states [35]. Additionally, nondegenerate three-level lasers—with a gain medium composed of three-level atoms in a cascade configuration—have become an attractive candidate for generating strong entangled photon pairs [36]. In these lasers, quantum coherence between the upper and lower levels of a single three-level atom serves as a fundamental component. This coherence can be achieved by initially preparing

the atoms in a coherent superposition of the upper and lower levels (injected coherence process) [37], by coupling the two levels using a strong external field (driven coherence process) [38], or by combining both methods [39].

Several theoretical proposals have shown that two spatially separated movable mirrors can become entangled by transferring entanglement from a correlated-emission laser in a doubly resonant cavity. For instance, Zhou *et al.* [40] demonstrated that two optical modes can be entangled through interaction with three-level atoms in a cascade configuration, where atomic coherence is induced via the injected coherence process. They essentially showed that this generated entanglement can then be transferred to two movable mirrors via radiation pressure. In contrast, using the driven coherence process, Ge *et al.* [41] showed that two movable mirrors can also be entangled in the strong optomechanical coupling regime. Sete and Eleuch [33] employ both injected and driven coherence process to achieve entanglement between two movable mirrors in the adiabatic regime. Recently, various mechanisms to enhance the degree of mechanical entanglement in a doubly resonant optomechanical cavity have been analyzed, also within the adiabatic regime [42].

Motivated partly by the recent achievements in cavity optomechanics [43, 44] and atom-cavity quantum electrodynamics [45, 46]; and partly by the considerable attention that has recently been paid to EPR steering as the essential resource for asymmetric quantum information precessing tasks [5], we seek to extend the scope of discussion to investigate the possibility of implementing controllable one-way steering between two mechanical modes by transferring quantum coherence from a correlated-emission laser to these modes within a doubly resonant optomechanical cavity. We emphasize that optomechanical steering has been explored in several scenarios without the mediation of correlated-emission lasers [47, 48, 49]. However, achieving practical one-way steering with flexible controllability remains a demanding issue. Varying some intrinsic physical parameters such as the optical decay rate or/and the mechanical damping rate is often employed as a main method to adjust the direction of one-way steering [23, 48, 50, 51, 52]. Unfortunately, such method, not only induces additional losses and noises which affects the degree of the generated steering, but also makes the experimental operations more complicated since optical and mechanical losses are mainly related to the surface roughness, impurities and defects of mirror materials [30]. Therefore, it is worth to further investigate the manipulation of the direction of one-way steering through external mechanism, rather than via intrinsic mechanism.

In this paper, we propose a scheme to generate asymmetric Gaussian quantum steering between two spatially separated mechanical modes, labelled as m_1 and m_2, by transferring quantum coherence from correlated emission laser to them. Importantly, we show that the direction of one-way steering between the modes m_1 and m_2 could be controlled via either the temperatures of the mechanical baths or the input powers of the cavity drive lasers, which is more practicable in experimental operations.

The remainder of this paper is organized as follows. In Section 2, we introduce our model which involves a nondegenerate three-level laser interacting with two movable mirrors via radiation pressure force. In Section 3, using the master equation of two-mode laser coupled to a vacuum reservoir, we derive the linearized quantum Langevin equations that describe the optomechanical coupling between two cavity modes and two mechanical modes. We then use these equations to obtain the covariance matrix for the two mechanical modes in the steady-state. In Section 4, using the measure proposed in [29], we quantify and analyze the quantum steering between the two mechanical modes. Finally, in Section 5, we present our conclusions.

2 The Model and Hamiltonian of the Whole System

In Figure 1, we consider a nondegenerate three level laser with two vibrating mirrors. The gain medium of the laser is an ensemble of nondegenerate three-level atoms in a cascade configuration [36], where we use $|\ell_1\rangle$, $|\ell_2\rangle$, and $|\ell_3\rangle$ for denoting the upper, intermediate, and lower levels of a single atom, respectively. The atoms are initially pumped into a doubly resonant cavity at the lowest level $|\ell_3\rangle$ with a rate r_0, where the dipole-allowed transition $|\ell_1\rangle \to |\ell_2\rangle(|\ell_2\rangle \to |\ell_3\rangle)$ is assumed to be resonant with a cavity mode $c_1(c_2)$ having frequency $\nu_1(\nu_2)$ and decay rate $\kappa_1(\kappa_2)$. The jth cavity mode is driven by an external coherent laser of frequency ω_{L_j}, power $\wp_j$, and amplitude $\epsilon_j = \sqrt{2\kappa_j\wp_j/\hbar\omega_{L_j}}$. The dipole-forbidden transition $|\ell_1\rangle \leftrightarrow |\ell_3\rangle$ can be induced, for example, by a strong magnetic field [38]. The jth movable mirror is modeled as a quantum-mechanical mode, labelled as m_j, having an effective mass μ_j, frequency ω_{m_j}, damping rate γ_{m_j}, and annihilation operator b_j.

In the interaction picture, under the rotating-wave approximation (RWA), the Hamiltonian of the whole system writes $\mathcal{H}^{int} = \mathcal{H}^{int}_{af} + \mathcal{H}^{int}_{ac} + \mathcal{H}^{int}_{op}$, where $\mathcal{H}^{int}_{af} = \mathrm{i}\hbar \sum_{j=1}^{2} \varsigma_j \left(c_j|\ell_j\rangle\langle\ell_{j+1}| - |\ell_{j+1}\rangle\langle\ell_j|c_j^\dagger\right)$ describes the interaction between a single three-level atom and two modes of the cavity field, with $\varsigma_1(\varsigma_2)$ being the coupling strength between the transition $|\ell_1\rangle \to |\ell_2\rangle(|\ell_2\rangle \to |\ell_3\rangle)$ and the cavity mode of annihilation operator $c_1(c_2)$ [38]. Without affecting the generality of our study, we take identical spontaneous decay rates for both transitions $|\ell_1\rangle \to |\ell_2\rangle$ and $|\ell_2\rangle \to |\ell_3\rangle$, i.e., $\gamma_{1,2} = \gamma$, and identical coupling transitions, i.e., $\varsigma_{1,2} = \varsigma$. The Hamiltonian $\mathcal{H}^{int}_{ac} = \mathrm{i}\hbar\frac{\Omega}{2}(|\ell_1\rangle\langle\ell_3| - |\ell_3\rangle\langle\ell_1|)$ corresponds to the generation of atomic coherence between the lower level $|\ell_1\rangle$ and the upper level $|\ell_3\rangle$ via an external driving field of strength Ω. The optomechanical Hamiltonian $\mathcal{H}^{int}_{op}$ is given by

$$\mathcal{H}^{int}_{op} = \sum_{j=1}^{2} \left[\hbar\Delta_j c_j^\dagger c_j + \hbar\omega_{m_j} b_j^\dagger b_j - \hbar g_j c_j^\dagger c_j (b_j^\dagger + b_j) + \mathrm{i}\hbar\epsilon_j (c_j^\dagger e^{i\Delta'_j} - c_j e^{-i\Delta'_j})\right], \tag{1}$$

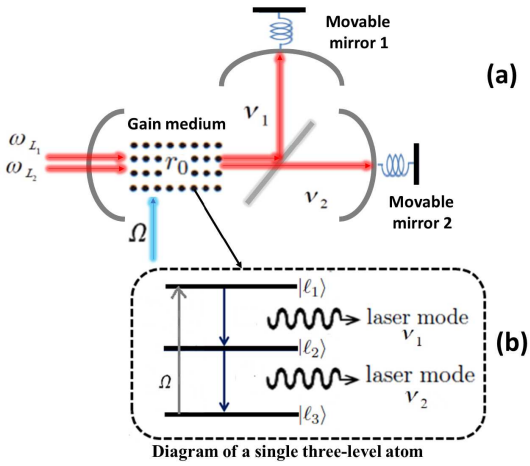

Figure 1: (a) Scheme of generating quantum steering of two movable mirrors inside a doubly resonant optomechanical cavity. The gain medium in the cavity is driven by an external field of strength Ω and interacts with two cavity modes of frequencies ν_1 and ν_2. The jth cavity mode is driven by an external laser of frequency ω_{L_j}, and coupled to its corresponding movable mirror via radiation pressure force. (b) Schematic diagram of a nondegenerate three-level laser coupled to a vacuum reservoir. r_0 is the rate at which the atoms are injected into the cavity. $|\ell_1\rangle$, $|\ell_2\rangle$, and $|\ell_3\rangle$ denote the upper, intermediate, and lower energy levels of a single three-level atom, respectively. The dipole-allowed transition $|\ell_1\rangle \to |\ell_2\rangle(|\ell_2\rangle \to |\ell_3\rangle)$ is assumed to be resonant with the cavity mode of frequency $\nu_1(\nu_2)$, while the dipole-forbidden transition $|\ell_1\rangle \leftrightarrow |\ell_3\rangle$ can be induced by a resonant semiclassical laser field of strength Ω. $\nu_1(\nu_2)$ denote the frequency of the laser mode generated during the transition $|\ell_1\rangle \to |\ell_2\rangle(|\ell_2\rangle \to |\ell_3\rangle)$.

where Δ_j is the jth laser detuning induced by radiation pressure force [30]. The optomechanical coupling strength between the jth cavity mode and its corresponding mechanical mode is given by $g_j = (\nu_j/l_j)\sqrt{\hbar/\mu_j\omega_{m_j}}$, with l_j being the jth cavity length at equilibrium. Finally, $\Delta'_j = \nu_j - \Delta_j - \omega_{L_j}$ denotes the effective detuning of the jth cavity-driving field.

The dynamics of the reduced density operator $\rho_{o_1o_2} \equiv \rho$ of two-mode laser o_1 and o_2 generated during the first and second transitions respectively, can be described by the master equation [11, 53]

$$\frac{d\rho}{dt} = \frac{-\mathrm{i}}{\hbar}\mathrm{Tr}_{\mathrm{sa}}[\mathcal{H}_{af}^{int} + \mathcal{H}_{ac}^{int}, \rho_{(\mathrm{sa},o_1o_2)}] + \sum_{j=1,2}\kappa_j\mathcal{L}[c_j]\rho, \tag{2}$$

where $\rho_{(\mathrm{sa},o_1o_2)}$ is the density operator describing the two-mode laser together with a single three-level atom, and $\mathrm{Tr}_{\mathrm{sa}}$ denotes the partial trace over the state of a single atom. The Lindblad operator $\mathcal{L}[c_j]\rho = 2c_j\rho c_j^\dagger - c_j^\dagger c_j\rho - \rho c_j^\dagger c_j$ is added to take into account the coupling between the laser modes and the vacuum reservoir [54]. In the good cavity limit where $\kappa_j \ll \gamma_j$, the atoms reach their steady state much faster than the cavity modes, then the dynamics of the atoms can be eliminated adiabatically. Under such condition, El Qars [11] has derived the master equation of the reduced density operator for two-mode laser coupled to two-mode squeezed vacuum reservoir. Following the standard methods of laser theory [53, 55], one can show that Equation (2) would be (details of the calculations are given in Appendix B)

$$\begin{aligned}\frac{d\rho}{dt} &= \Xi_{11}\left(2c_1^\dagger\rho c_1 - c_1c_1^\dagger\rho - \rho c_1c_1^\dagger\right) + \Xi_{22}\left(2c_2\rho c_2^\dagger - c_2^\dagger c_2\rho - \rho c_2^\dagger c_2\right)\\ &\quad -\Xi_{12}c_1c_2\rho - \Xi_{21}\rho c_1c_2 + (\Xi_{12}+\Xi_{21})c_2\rho c_1\\ &\quad -\Xi_{12}\rho c_1^\dagger c_2^\dagger - \Xi_{21}c_1^\dagger c_2^\dagger\rho + (\Xi_{12}+\Xi_{21})c_1^\dagger\rho c_2^\dagger\\ &\quad +\kappa_1\left(2c_1\rho c_1^\dagger - c_1^\dagger c_1\rho - \rho c_1^\dagger c_1\right) + \kappa_2\left(2c_2\rho c_2^\dagger - c_2^\dagger c_2\rho - \rho c_2^\dagger c_2\right),\end{aligned} \tag{3}$$

where

$$\Xi_{11} = \frac{3\mathcal{A}}{8}\frac{\Omega^2\gamma^2}{(\Omega^2+\gamma^2)(\frac{\Omega^2}{4}+\gamma^2)},\ \Xi_{22} = \frac{\mathcal{A}}{2}\frac{\gamma^2}{(\Omega^2+\gamma^2)}, \tag{4}$$

$$\Xi_{12} = -\frac{\mathcal{A}}{2}\frac{\Omega\gamma}{(\Omega^2+\gamma^2)},\quad \text{and}\quad \Xi_{21} = \frac{\mathcal{A}}{8}\frac{\Omega\gamma(\Omega^2-2\gamma^2)}{(\Omega^2+\gamma^2)(\frac{\Omega^2}{4}+\gamma^2)}, \tag{5}$$

with $\mathcal{A} = 2r_0\varsigma^2/\gamma^2$ being the linear gain coefficient that quantifies the rate at which the atoms are injected into the cavity [36]. In Equation (3) the term proportional to $\Xi_{11}(\Xi_{22})$ corresponds to the gain(loss) of the first(second) laser mode, while the next six terms traduce the coupling between the two emitted laser modes due to atomic coherence induced by the driven field of strength Ω. We emphasize that such terms are responsible for the creation of quantum correlations between the two generated laser modes [36]. In this work, we will exploit these correlations to produce asymmetric Gaussian quantum steering between two non-interacting movable mirrors. Finally, the two last terms in Equation (3) proportional to κ_1 and κ_2 traduce the damping of the two-mode laser in the vacuum reservoir.

3 Quantum Langevin Equations for the Optomechanical Subsystem

Now we derive the quantum Langevin equations for the two cavity modes $c_{1,2}$ and the two mechanical modes $m_{1,2}$. For this, we assume the coupling between a single atom and the cavity modes to be much stronger than the optomechanical coupling which allows us to obtain the quantum Langevin equations for the atom–cavity subsystem and the optomechanical subsystem separately. The quantum Langevin equations for the cavity modes could be derived from Equation (3) using the formula $\frac{d}{dt}\langle\mathcal{O}\rangle = \mathrm{Tr}\left(\frac{d\rho}{dt}\mathcal{O}\right)$ for $\mathcal{O}_j \equiv c_j$ and removing the bracket $\langle . \rangle$ from the resulting equations, and next adding appropriate noise operators $\digamma_j$ with zero mean value ($\langle \digamma_j \rangle = 0$) . Therefore, we get (details of the calculations are given in Appendix C)

$$\partial_t c_1 = -\left(\kappa_1 - \Xi_{11}\right) c_1 + \Xi_{12} c_2^\dagger + \digamma_1, \tag{6}$$

$$\partial_t c_2 = -\left(\kappa_2 + \Xi_{22}\right) c_2 - \Xi_{21} c_1^\dagger + \digamma_2, \tag{7}$$

where the time-domain correlation functions of the noise operators $\digamma_1$ and $\digamma_2$ can be obtained from Einstein's relation [56]

$$2\langle \mathcal{D}_{\mathcal{O}_1\mathcal{O}_2}\rangle = \frac{d\langle \mathcal{O}_1\mathcal{O}_2\rangle}{dt} - \langle\left(\dot{\mathcal{O}}_1 - \digamma_{\mathcal{O}_1}\right)\mathcal{O}_2\rangle - \langle\mathcal{O}_1\left(\dot{\mathcal{O}}_2 - \digamma_{\mathcal{O}_2}\right)\rangle, \tag{8}$$

with $\langle \mathcal{D}_{\mathcal{O}_1\mathcal{O}_2}\rangle$ being the diffusion coefficient for $\mathcal{O}_j \equiv c_j$, and $\digamma_{\mathcal{O}_1}$ and $\digamma_{\mathcal{O}_2}$ belong to their corresponding noise operators. Using Equation (8) and the equations for the second-order moments of the laser modes operators c_j together with $\langle \digamma_{\mathcal{O}_1}(t)\digamma_{\mathcal{O}_2}(t')\rangle = 2\langle \mathcal{D}_{\mathcal{O}_1\mathcal{O}_2}\rangle\delta(t-t')$, the non-vanishing correlation functions for the operators $\digamma_1$ and $\digamma_2$ are

$$\langle \digamma_1^\dagger(t)\digamma_1(t')\rangle = 2\Xi_{11}\delta(t-t'), \tag{9}$$

$$\langle \digamma_1(t)\digamma_1^\dagger(t')\rangle = 2\kappa_1\delta(t-t'), \tag{10}$$

$$\langle \digamma_2(t)\digamma_2^\dagger(t')\rangle = 2\left(\kappa_2 + \Xi_{22}\right)\delta(t-t'), \tag{11}$$

$$\langle \digamma_1^\dagger(t)\digamma_2^\dagger(t')\rangle = \langle \digamma_2(t)\digamma_1(t')\rangle = -2\left(\Xi_{12} + \Xi_{21}\right)\delta(t-t'). \tag{12}$$

We emphasize that since the quantum system at hand is intrinsically open, consequently it is inevitably affected by the environmental noises. Then, the quantum noise operators $\digamma_1$ and $\digamma_2$, appeared in Equations (6) and (7), are added to take into account the effect of the noise resulting from the coupling between the laser modes and the vacuum reservoir.

Now, a more general dynamics of the laser modes can be obtained by adding the contribution of the optomechanical Hamiltonian (1) in Equations (6) and (7). To do this, we add $\frac{1}{i\hbar}[c_1, \mathcal{H}_{op}^{int}]$ and $\frac{1}{i\hbar}[c_2, \mathcal{H}_{op}^{int}]$, respectively, in the right hand side of Equations (6) and (7). Then, we get

$$\partial_t c_1 = -\left(\kappa_1 - \Xi_{11} + i\Delta_1\right) c_1 + \Xi_{12} c_2^\dagger + i g_1 c_1 (b_1^\dagger + b_1) + \epsilon_1 e^{i\Delta_1'} + \digamma_1, \tag{13}$$

$$\partial_t c_2 = -\left(\kappa_2 + \Xi_{22} + i\Delta_2\right) c_2 - \Xi_{21} c_1^\dagger + i g_2 c_2 (b_2^\dagger + b_2) + \epsilon_2 e^{i\Delta_2'} + \digamma_2. \tag{14}$$

The two mechanical modes are also affected by damping and noise processes, due to the fact that each of them interacts with its own thermal bath. Therefore, their dynamics can be obtained by adopting the quantum Langevin equations treatment, in which the Heisenberg equation associated with the Hamiltonian (1) is supplemented with mechanical damping and Brownian noise terms, i.e., $\partial_t b_j = \frac{1}{i\hbar}[b_j, \mathcal{H}_{op}^{int}] - \gamma_{m_j} b_j + \sqrt{2\gamma_{m_j}}\zeta_j$ [57]. Then, we obtain

$$\partial_t b_j = -\left(\gamma_{m_j} + i\omega_{m_j}\right) b_j + i g_j c_j^\dagger c_j + \sqrt{2\gamma_{m_j}}\zeta_j, \text{ for } j = 1, 2, \tag{15}$$

where ζ_j denotes the Brownian noise operator, with zero-mean value, that affects the jth mechanical mode at temperature T_j. In general, the operator ζ_j is not δ-correlated, exhibiting a non-Markovian correlation property

between two instants t and t' [58]. However, large mechanical quality factor $\mathcal{Q}_{m_j} = \omega_{m_j}/\gamma_{m_j} \gg 1$ allows us recovering the Markovian process. Then, we have [59]

$$\langle \zeta_j^\dagger(t)\zeta_j(t')\rangle = n_{\mathrm{th},j}\delta(t-t') \text{ for } j=1,2, \tag{16}$$

$$\langle \zeta_j(t)\zeta_j^\dagger(t')\rangle = (n_{\mathrm{th},j}+1)\,\delta(t-t'), \tag{17}$$

where $n_{\mathrm{th},j} = (e^{\hbar\omega_{m_j}/k_B T_j}-1)^{-1}$ is the jth mean thermal phonon number and k_B is the Boltzmann constant. We emphasize that non-Markovian evolution of EPR steering has been recently observed experimentally in [60].

Due to the quadratic terms $c_j^\dagger c_j$, $c_j b_j^\dagger$ and $c_j b_j$, the nonlinear quantum Langevin equations [(13)-(15)] cannot be solved analytically. However, assuming bright pump fields, one can linearize the dynamics around the steady state by adopting standard method of quantum optics [58]. To realise this, we first choose a rotating frame defined as $\tilde{c}_j = c_j e^{-i\Delta_j' t}$, next we write each Heisenberg operator $\mathcal{O}_j \equiv \tilde{c}_j, b_j$ as a complex steady state value $\langle\mathcal{O}_j\rangle$ plus a small fluctuation $\delta\mathcal{O}_j$ with vanishing-mean value, i.e., $\mathcal{O}_j = \langle\mathcal{O}_j\rangle + \delta\mathcal{O}_j$. In the choosing rotating frame, the obtained equations for the fluctuations $\delta\tilde{c}_1$ and $\delta\tilde{c}_2$ as well as the mean values $\langle\tilde{c}_1\rangle$ and $\langle\tilde{c}_2\rangle$ will be coupled through terms proportional to $\Xi_{12}e^{-i(\Delta_1'+\Delta_2')t}$ and $\Xi_{21}e^{-i(\Delta_1'+\Delta_2')t}$. Then, by performing the RWA that allows us to drop the highly oscillating terms with the factor $e^{-i(\Delta_1'+\Delta_2')t}$, solely in the quantum Langevin equations of $\langle\tilde{c}_j\rangle$, and next setting the time derivatives in the resulting equations, we obtain $\langle b_j\rangle^* + \langle b_j\rangle = \frac{|\langle\tilde{c}_j\rangle|^2}{\omega_{m_j}}$ and $\langle\tilde{c}_j\rangle = \frac{\epsilon_j}{\kappa_j + i\Delta_j' + (-1)^j\Xi_{jj}}$, where $\Delta_j' = \nu_j - \omega_{L_j} - g_j\left(\langle b_j\rangle^* + \langle b_j\rangle\right)$ denotes the effective detuning of the jth cavity mode frequency. Hence, it follows that the mean frequency shift Δ_j, introduced in Equation (1), is given by $\Delta_j = g_j\left(\langle b_j\rangle^* + \langle b_j\rangle\right)$.

Now, transforming back to the original rotating frame, i.e., $\delta c_j = \delta\tilde{c}_j e^{i\Delta_j' t}$ and introducing $\delta\tilde{b}_j = \delta b_j e^{-i\omega_j t}$, one has

$$\partial_t\delta c_1 = -\bar{\kappa}_1\delta c_1 + \Xi_{12}\delta c_2^\dagger + iG_1\left(\delta\tilde{b}_1 e^{-i\left(\omega_{m_1}-\Delta_1'\right)t} + \delta\tilde{b}_1^\dagger e^{i\left(\omega_{m_1}+\Delta_1'\right)t}\right) + \digamma_1, \tag{18}$$

$$\partial_t\delta c_2 = -\bar{\kappa}_2\delta c_2 - \Xi_{21}\delta c_1^\dagger + iG_2\left(\delta\tilde{b}_2 e^{-i\left(\omega_{m_2}-\Delta_2'\right)t} + \delta\tilde{b}_2^\dagger e^{i\left(\omega_{m_2}+\Delta_2'\right)t}\right) + \digamma_2, \tag{19}$$

$$\partial_t\delta\tilde{b}_j = -\gamma_{m_j}\delta\tilde{b}_j + iG_j^*\delta c_j e^{i\left(\omega_{m_j}-\Delta_j'\right)t} + iG_j\delta c_j^\dagger e^{i\left(\omega_{m_j}+\Delta_j'\right)t} + \sqrt{2\gamma_{m_j}}\tilde{\zeta}_j, \text{ for } j=1,2, \tag{20}$$

where $\bar{\kappa}_j = \kappa_j + (-1)^j\Xi_{jj}$, $\tilde{\zeta}_j = \zeta_j e^{i\omega_{m_j}t}$, and $G_j = g_j\langle\tilde{c}_j\rangle$ being the effective many-photon optomechanical coupling [30]. Notice that one can easily verify that the operator ζ_j fulfills the same correlation properties given by Equations (16) and (17).

When the input lasers are scattered at the anti-Stokes sidebands, i.e., $\Delta_j' = +\omega_{m_j}$, the operators δc_j and $\delta\tilde{b}_j$ will be coupled via a beam-splitter-like process [58], which is shown to be a very stable regime [41]. Importantly, although there is no direct interaction between the two mechanical modes m_1 and m_2, entanglement between them could be generated via transferring quantum correlations from the correlated-emission laser to the state of the two movable mirrors. Indeed, under the condition $\kappa_j \gg \gamma_{m_j}$, which is considered in this work, the effective coupling between the modes m_1 and m_2 can be obtained by eliminating adiabatically the dynamics of the cavity modes from Equations (18) and (19) and replacing into Equation (20). Then, in the resulting equations, the two mechanical modes will be coupled to each other via a parametric down conversion process which leads to entanglement between them [58].

Using $\Delta_j' = +\omega_{m_j}$ for $j=1,2$ in Equations [(18)-(20)], and assuming that $\omega_{m_j} \gg \kappa_j$, therefore the RWA allows us to neglect the terms rapidly oscillating at $+2\omega_{m_j}$ [10], hence we get

$$\partial_t\delta c_1 = -\bar{\kappa}_1\delta c_1 + \Xi_{12}\delta c_2^\dagger + iG_1\delta\tilde{b}_1 + \digamma_1, \tag{21}$$

$$\partial_t\delta c_2 = -\bar{\kappa}_2\delta c_2 - \Xi_{21}\delta c_1^\dagger + iG_2\delta\tilde{b}_2 + \digamma_2, \tag{22}$$

$$\partial_t\delta\tilde{b}_j = -\gamma_{m_j}\delta\tilde{b}_j + iG_j^*\delta c_j + \sqrt{2\gamma_{m_j}}\tilde{\zeta}_j \text{ for } j=1,2 \tag{23}$$

Using the dimenssionless position and momentum fluctuations of the jth mechanical(cavity) mode $\delta\tilde{q}_{m_j} = (\delta\tilde{b}_j^\dagger + \delta\tilde{b}_j)/\sqrt{2}$ and $\delta\tilde{p}_{m_j} = i(\delta\tilde{b}_j^\dagger - \delta\tilde{b}_j)/\sqrt{2}$ $\left(\delta q_{c_j} = (\delta c_j^\dagger + \delta c_j)/\sqrt{2} \text{ and } \delta p_{c_j} = i(\delta c_j^\dagger - \delta c_j)/\sqrt{2}\right)$ with the input noises $\tilde{q}_{m_j}^{in} = (\tilde{\zeta}_j^\dagger + \tilde{\zeta}_j)/\sqrt{2}$ and $\tilde{p}_{m_j}^{in} = i(\tilde{\zeta}_j^\dagger - \tilde{\zeta}_j)/\sqrt{2}$ $\left(q_{c_j}^{in} = (\digamma_j^\dagger + \digamma_j)/\sqrt{2} \text{ and } p_{c_j}^{in} = i(\digamma_j^\dagger - \digamma_j)/\sqrt{2}\right)$, and Equations [(21)-(23)], we obtain the linear quantum Langevin equations in the RWA in a compact form as $\partial_t\mathcal{U} = \mathcal{K}\mathcal{U} + \mathcal{N}$, with $\mathcal{U}^{\mathrm{T}} = (\delta\tilde{q}_{m_1}, \delta\tilde{p}_{m_1}, \delta\tilde{q}_{m_2}, \delta\tilde{p}_{m_2}, \delta q_{c_1}, \delta q_{c_1}, \delta q_{c_2}, \delta q_{c_2})$, $\mathcal{N}^{\mathrm{T}} = (\sqrt{2\gamma_{m_1}}\tilde{q}_{m_1}^{in}, \sqrt{2\gamma_{m_1}}\tilde{p}_{m_1}^{in}, \sqrt{2\gamma_{m_2}}\tilde{q}_{m_2}^{in}, \sqrt{2\gamma_{m_2}}\tilde{p}_{m_2}^{in}, q_{c_1}^{in}, p_{c_1}^{in}, q_{c_2}^{in}, p_{c_2}^{in})$

and the kernel $\mathcal{K}$ is given by

$$\mathcal{K}=\begin{pmatrix} -\gamma_{m_1} & 0 & 0 & 0 & 0 & -G_1 & 0 & 0 \\ 0 & -\gamma_{m_1} & 0 & 0 & G_1 & 0 & 0 & 0 \\ 0 & 0 & -\gamma_{m_2} & 0 & 0 & 0 & 0 & -G_2 \\ 0 & 0 & 0 & -\gamma_{m_2} & 0 & 0 & G_2 & 0 \\ 0 & -G_1 & 0 & 0 & -\bar{\kappa}_1 & 0 & \Xi_{12} & 0 \\ G_1 & 0 & 0 & 0 & 0 & -\bar{\kappa}_1 & 0 & -\Xi_{12} \\ 0 & 0 & 0 & -G_2 & -\Xi_{21} & 0 & -\bar{\kappa}_2 & 0 \\ 0 & 0 & G_2 & 0 & 0 & \Xi_{21} & 0 & -\bar{\kappa}_2 \end{pmatrix}, \tag{24}$$

where the effective optomechanical coupling G_j is chosen, for simplicity, to be $G_j = g_j\,|\langle\tilde{c}_j\rangle|$.

The solution of the linearized quantum Langevin equations can be obtained as $\mathcal{U}(t) = \mathcal{M}(t)\mathcal{U}(0)+\int_0^{t'} dt\mathcal{M}(t)\mathcal{N}(t'-t)$ where $\mathcal{M}(t) = \exp(\mathcal{K}t)$ [61]. The system is stable if and only if all real parts of the eigenvalues of the matrix $\mathcal{K}$ are negative, so that $\mathcal{M}(t\to\infty) = 0$. The stability conditions can be derived applying the Routh-Hurwitz criterion [62], where details of the calculations are given in Appendix A.

Since the dynamics of the system is linearized around the steady state, and the operators $\tilde{\hat{\zeta}}_j^{in}$ and $\digamma_j$ are zero-mean quantum Gaussian noises, therefore the steady state of the quantum fluctuations is a zero-mean four-mode Gaussian state described by its 8×8 covariance matrix ϑ of elements $\vartheta_{ii'} = (\langle\mathcal{U}_i(\infty)\mathcal{U}_{i'}(\infty) + \mathcal{U}_{i'}(\infty)\mathcal{U}_i(\infty)\rangle)/2$ [61]. When the system is stable, we obtain

$$\vartheta_{ii'} = \sum_{k,k'}\int_0^\infty ds\int_0^\infty ds'_{ik}\mathcal{M}(s)\mathcal{M}_{i'k'}(s')\Phi_{kk'}(s-s'), \tag{25}$$

where $\Phi_{kk'}(s-s') = (\langle\mathcal{N}_k(s)\mathcal{N}_{k'}(s') + \mathcal{N}_{k'}(s')\mathcal{N}_k(s)\rangle)/2 = \mathcal{R}_{kk'}\delta(s-s')$, with $\mathcal{R}_{kk'}$ being the elements of the diffusion matrix $\mathcal{R}$ [61]. Using the correlation properties of the operators $\tilde{\hat{\zeta}}_j^{in}$ and $\digamma_j$, we show that $\mathcal{R} = \mathcal{R}_m \oplus \mathcal{R}_c$ with $\mathcal{R}_m = (\gamma_{m_1}(2n_{\text{th},1}+1)\mathbb{1}_2 \oplus \gamma_{m_2}(2n_{\text{th},2}+1)\mathbb{1}_2)$ and

$$\mathcal{R}_c = \begin{pmatrix} \kappa_1+\Xi_{11} & 0 & -\frac{\Xi_{12}+\Xi_{21}}{2} & 0 \\ 0 & \kappa_1+\Xi_{11} & 0 & \frac{\Xi_{12}+\Xi_{21}}{2} \\ -\frac{\Xi_{12}+\Xi_{21}}{2} & 0 & \kappa_2+\Xi_{22} & 0 \\ 0 & \frac{\Xi_{12}+\Xi_{21}}{2} & 0 & \kappa_2+\Xi_{22} \end{pmatrix}. \tag{26}$$

When the stability conditions are satisfied, Equation (25) becomes $\vartheta = \int_0^\infty ds\mathcal{M}(s)\mathcal{R}\mathcal{M}(s)^{\mathrm{T}}$ which is equivalent to the Lyapunov equation [58]

$$\mathcal{K}\vartheta + \vartheta\mathcal{K}^{\mathrm{T}} = -\mathcal{R}. \tag{27}$$

The covariance matrix ϑ, solution of Equation (27), can be expressed as

$$\vartheta = [\vartheta_{ij}]_{8\times 8} = \begin{pmatrix} \vartheta_{m_1} & \vartheta_{m_{12}} & \vartheta_{m_1c_1} & \vartheta_{m_1c_2} \\ \vartheta_{m_{12}}^{\mathrm{T}} & \vartheta_{m_2} & \vartheta_{m_2c_1} & \vartheta_{m_2c_2} \\ \vartheta_{m_1c_1}^{\mathrm{T}} & \vartheta_{m_2c_1}^{\mathrm{T}} & \vartheta_{c_1} & \vartheta_{c_{12}} \\ \vartheta_{m_1c_2}^{\mathrm{T}} & \vartheta_{m_2c_2}^{\mathrm{T}} & \vartheta_{c_{12}}^{\mathrm{T}} & \vartheta_{c_2} \end{pmatrix}, \tag{28}$$

where the 2×2 blocks matrices ϑ_{m_1} and ϑ_{m_2} (ϑ_{c_1} and ϑ_{c_2}) describe the first and second mechanical(cavity) modes, while the correlations between them are described by the matrix $\vartheta_{m_{12}}(\vartheta_{c_{12}})$. The matrix $\vartheta_{m_ic_j}$ $(i,j\in\{1,2\})$ represents the correlations between the ith mechanical mode and the jth cavity mode.

As mentioned above, in this work we exploit the entanglement between the two-mode laser emitted during the cascade transitions of the atomic system to generate asymmetric Gaussian quantum steering between the two mechanical modes m_1 and m_2, where their corresponding covariance matrix ϑ_m can be deduced by tracing over the cavity modes elements in Equation (28). Hence, we get

$$\vartheta_m = \begin{pmatrix} \vartheta_{m_1} & \vartheta_{m_{12}} \\ \vartheta_{m_{12}}^{\mathrm{T}} & \vartheta_{m_2} \end{pmatrix}. \tag{29}$$

4 Gaussian Quantum Steering

A bipartite state ϱ_{AB}, shared between two observers Alice and Bob, is steerable from $A\to B$, i.e., Alice can steer Bob's states via implementing a set of measurements M_A on her side, if it is impossible for every pair of local observables $r_A\in M_A$ on A and r_B (arbitrary) on B, with outcomes r'_A and r'_B, respectively, to write the joint probability as $p(r'_A, r'_B|r_A, r_B, \varrho_{AB}) = \sum_\alpha p_\alpha p(r'_A|r_A,\alpha)p(r'_B|r_B,\varrho_\alpha)$. In other words, at least one measurement

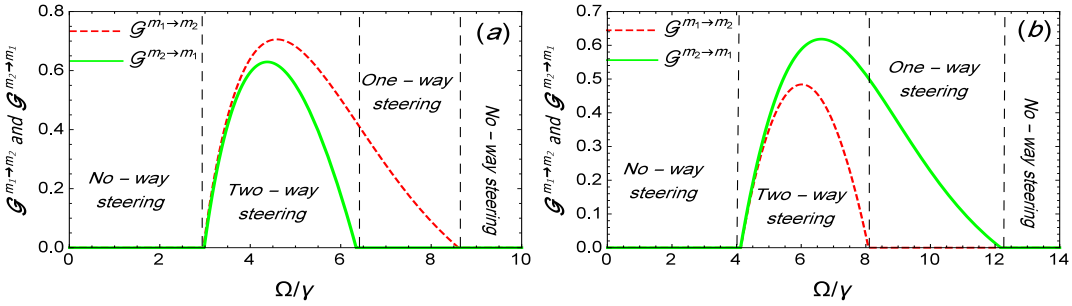

Figure 2: Plot of the Gaussian steerabilities $\mathcal{G}^{m_1\to m_2}$ (red dashed curve) and $\mathcal{G}^{m_2\to m_1}$ (green solid curve) versus the normalized driving field strength Ω/γ using $\kappa = 2\pi \times 215$ kHz, $\gamma_m = 2\pi \times 140$ Hz, $\omega_m = 2\pi \times 947$ kHz, $G_{1,2}/\omega_m = 0.25$, $\gamma = 1.7$ MHz, and $\mathcal{A} = 250$ MHz. We used $n_{\text{th},1} = 15$ which corresponds to $T_1 = 0.7$ mK and $n_{\text{th},2} = 5$ which corresponds to $T_2 = 0.3$ mK in (a), while we used $n_{\text{th},1} = 5$ and $n_{\text{th},2} = 15$ in (b). The stronger two-way steering ($\mathcal{G}^{m_{1(2)}\to m_{2(1)}} > 0$) observed over a wide range of Ω/γ in panels (a) and (b) is demonstrated to be a fundamental resource required for teleporting a coherent state with fidelity beyond the nocloning threshold [23]. While, the different degree of steering in both directions $m_1 \rightleftarrows m_2$, including one-way steering behavior, is proved to provide the asymmetric guaranteed key rate achievable in a practical 1SDI-QKD [29]. We should mention that the temperatures T_1 and T_2 employed in this figure are around 1 mK, which has been achieved experimentally in [64] with mechanical frequency very close to that used in the present work.

pair r_A and r_B should violate this expression if p_α is fixed across all measurements with p_α and $p(r'_A|r_A,\alpha)$ are probability distributions and $p(r'_B|r_B,\varrho_\alpha)$ represents the conditional probability distribution corresponding to the extra condition of being evaluated on the state ϱ_α. It has been shown by Wiseman *et al.* [4] that an arbitrary bipartite Gaussian state $\varrho_{m_1m_2}$ with covariance matrix ϑ_m is steerable under Gaussian measurements implemented on party m_1 if and only if the expression $\vartheta_m + \mathrm{i}(\Pi_{m_1} \oplus \Pi_{m_2}) \geqslant \mathbf{0}$ is violated, with $\Pi_{m_1} = \begin{pmatrix} 0 & 0 \\ 0 & 0 \end{pmatrix}$ and $\Pi_{m_2} = \begin{pmatrix} 0 & 1 \\ -1 & 0 \end{pmatrix}$. On the basis of this constraint, Kogias *et al.* [29] have proposed a computable measure to quantify the amount by which the state $\varrho_{m_1m_2}$ is steerable under Gaussian measurements performed on party m_1, i.e.,

$$\mathcal{G}^{m_1\to m_2} := \max\left[0, -\sum_{j:\bar{\nu}_j^{m_2}<1} \ln\left\{\bar{\nu}_j^{m_2}\right\}\right], \tag{30}$$

with $\{\bar{\nu}_j^{m_2}\}$ being the symplectic spectra of the Schur complement $\vartheta_{m_2} - \vartheta_{m_{12}}^{\mathrm{T}}\vartheta_{m_1}^{-1}\vartheta_{m_{12}}$ of party m_1 in the matrix ϑ_m (29). Notice that $\mathcal{G}^{m_1\to m_2}$ is monotone under Gaussian local operations and classical communication, and it vanishes if the state $\varrho_{m_1m_2}$ is nonsteerable under Gaussian measurements implemented on m_1. When m_1 and m_2 are single modes, Equation (30) acquires the compact form $\mathcal{G}^{m_1\to m_2} = \max\left[0, \frac{1}{2}\ln\frac{\det\vartheta_{m_1}}{4\det\vartheta_m}\right]$ [29], where the steering from $m_2 \to m_1$ can be obtained by changing the roles of the modes m_1 and m_2 in Equation (30), i.e., $\mathcal{G}^{m_2\to m_1} = \max\left[0, \frac{1}{2}\ln\frac{\det\vartheta_{m_2}}{4\det\vartheta_m}\right]$. A nonzero value of $\mathcal{G}^{m_i\to m_j}$ means that the state $\varrho_{m_1m_2}$ is steerable from $m_i \to m_j$ under Gaussian measurements performed on mode m_i. Hence, three cases can be distinguished: (*1*) two-way steering, where the state $\varrho_{m_1m_2}$ is steerable in both directions $m_{i(j)} \to m_{j(i)}$, i.e., $\mathcal{G}^{m_{i(j)}\to m_{j(i)}} > 0$, (*2*) no-way steering, where $\mathcal{G}^{m_{i(j)}\to m_{j(i)}} = 0$, and (*3*) one-way steering, where the state $\varrho_{m_1m_2}$ is steerable solely in one direction, that is, $\mathcal{G}^{m_i\to m_j} > 0$ with $\mathcal{G}^{m_j\to m_i} = 0$. We emphasize that pure entangled states cannot in general display one-way steering behavior, since they can always be transformed into a symmetric form through a local basis change employing the Schmidt decomposition [29]. Moreover, exploiting the method of homodyne detection [61, 63], the covariance matrix (29) of the two mechanical modes m_1 and m_2 can be determined experimentally, which allows us to estimate numerically the steerabilities $\mathcal{G}^{m_{1(2)}\to m_{2(1)}}$.

Notice that varying the optical decay rates κ_1 and κ_2 is often employed as a main method to adjust the direction of one-way steering [23, 48, 50, 51, 52]. Such method, not only induces additional losses and noises which affects the degree of the generated steering, but also makes the experimental operations more complicated since the optical losses are mainly related to the surface roughness, impurities and defects of mirror materials [30]. In the scheme that we consider here, we will show that the direction of one-way steering could be controlled via the effective optomechanical coupling strengths G_1 and G_2 or the values of the means thermal occupations $n_{\text{th},1}$ and $n_{\text{th},2}$. The first method could be achieved via controlling the lasers drive powers $\wp_1$ and $\wp_2$, while the second could be achieved via adjusting the temperatures T_1 and T_2 of the mechanical baths, which is more practicable in experimental operations.

For numerical estimation of the steerabilities $\mathcal{G}^{m_1\to m_2}$ and $\mathcal{G}^{m_2\to m_1}$, we have taken identical mirrors with mass $\mu_{1,2} = 145$ ng, frequency $\omega_{m_{1,2}} = 2\pi \times 947$ kHz, and damping rate $\gamma_{m_{1,2}} = 2\pi \times 140$ Hz. The cavities,

having identical decay rates $\kappa_{1,2} = 2\pi \times 215$ kHz, equilibrium lengths $\ell_1 = 0.532$ mm and $\ell_2 = 0.405$ mm, frequencies $\nu_1 = 2\pi \times 4.32 \times 10^{14}$ Hz and $\nu_2 = 2\pi \times 4.33 \times 10^{14}$ Hz, are pumped by input lasers of frequencies $\omega_{L_1} = 2\pi \times 3.7 \times 10^{14}$ Hz and $\omega_{L_2} = 2\pi \times 2.82 \times 10^{14}$ Hz [43, 44]. The atomic decay rates $\gamma_{1,2} = 1.7$ MHz, the atom–field coupling strengths $\varsigma_{1,2} = 15$ MHz, the rate at which the atoms are injected into the cavity $r_0 = 1.6$ MHz, so that the linear gain coefficient $\mathcal{A} = 2r_0\varsigma^2/\gamma^2 \approx 250$ MHz [41].

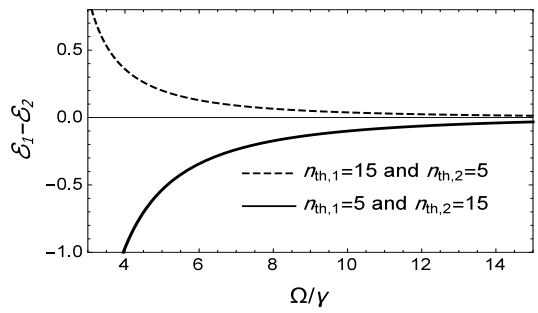

Figure 3: Plot of the difference $\mathcal{E}_1 - \mathcal{E}_2$, in units of $\frac{1}{2}\hbar\omega_m$, where $\mathcal{E}_j = \frac{\hbar\omega_m}{2}(\langle\delta\tilde{q}^2_{m_j}\rangle + \langle\delta\tilde{p}^2_{m_j}\rangle)$ is the energy of the jth mechanical mode. The black dashed(solid) curve is plotted under the same conditions as in Figure 2(a)(Figure 2(b)).

In Figure 2 we plot the effect of the normalized driving field strength Ω/γ on the steerabilities $\mathcal{G}^{m_1\to m_2}$ and $\mathcal{G}^{m_2\to m_1}$ using $G_{1,2}/\omega_m = 0.25$ for the effective optomechanical coupling strengths. For the thermal occupancies, we used $n_{\text{th},1} = 15$ which corresponds to $T_1 = 0.7$ mK and $n_{\text{th},2} = 5$ which corresponds to $T_2 = 0.3$ mK in Figure 2(a), while we used $n_{\text{th},1} = 5$ and $n_{\text{th},2} = 15$ in Figure 2(b). Even though there is no direct interaction between the mechanical modes m_1 and m_2, Gaussian quantum steering could be detected between them due to quantum coherence transfer from the three-level laser to the state $\varrho_{m_1m_2}$ via the optomechanical coupling. Manifestly, there exists a minimum strength of the driving field, and then a minimum of atomic coherence for which the state $\varrho_{m_1m_2}$ is steerable. Furthermore, by increasing gradually the drive amplitude Ω—from the required minimum—the steerabilities $\mathcal{G}^{m_1\to m_2}$ and $\mathcal{G}^{m_2\to m_1}$ arise and undergo a resonance-like behavior. This indicates that the steering between the two mirrors can be controlled with the driven filed that couples the atomic coherence to the cavity modes. Essentially, Figure 2 shows that inferring about the mechanical mode m_i based on measurements performed on mode m_j is fully different from the reverse operation, i.e., $\mathcal{G}^{m_1\to m_2} \neq \mathcal{G}^{m_2\to m_1}$, where two-way steering (i.e., $\mathcal{G}^{m_{1(2)}\to m_{2(1)}} > 0$) and one-way steering (i.e., $\mathcal{G}^{m_i\to m_j} > 0$ and $\mathcal{G}^{m_j\to m_i} = 0$ for $i \neq j = 1, 2$) could be observed. From an operational point of view, one-way steering observed from $m_i \to m_j$ implies that the observer owning mode m_i and that owning mode m_j can perform identical Gaussian measurements on their own modes, however get conflicting outcomes. Moreover, the former can convince the latter that the state $\varrho_{m_1m_2}$ is entangled, while the converse is not true. This is partly due to the asymmetric form of the matrix ϑ (29), where $\det\vartheta_{m_1} \neq \det\vartheta_{m_2}$, and partly due to the definition of the aspect of quantum steering in terms of the EPR paradox [4, 29]. We notice that asymmetric steering is proved to supply security in 1SDI-QKD protocol, where the measurement apparatus of one device is untrusted [29].

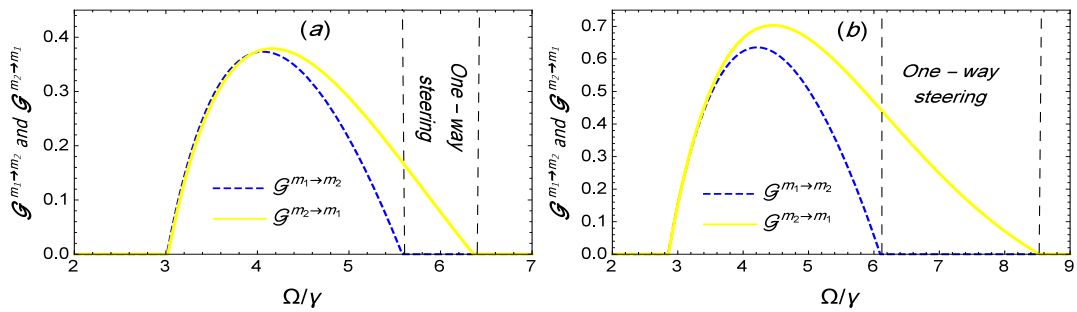

Figure 4: Plot of the Gaussian steerabilities $\mathcal{G}^{m_1\to m_2}$ (blue dashed curve) and $\mathcal{G}^{m_2\to m_1}$ (yellow solid curve) versus the normalized driving field strength Ω/γ using $\kappa = 2\pi \times 215$ kHz, $\gamma_m = 2\pi \times 140$ Hz, $\omega_m = 2\pi \times 947$ kHz, $\mathcal{A} = 250$ MHz, and $n_{\text{th},1,2} = 15$. For the effective optomechanical coupling strengths, we used $G_{1,2}/\omega_m = G/\omega_m = 0.25$ in (a) and $G/\omega_m = 0.35$ in (b). This figure clearly shows the advantage of the mediation of the effective optomechanical coupling strength in observing one-way steering through a wide range of Ω/γ, which allows us the implementation of more one-way quantum information tasks.

Strikingly, in Figure 2(a) where we used $n_{\text{th},1} = 15$ and $n_{\text{th},2} = 5$, the steering $\mathcal{G}^{m_1\to m_2}$ remains greater than $\mathcal{G}^{m_2\to m_1}$ and one-way steering is occurred from $m_1 \to m_2$. While, $\mathcal{G}^{m_1\to m_2}$ remains less than $\mathcal{G}^{m_2\to m_1}$ and one-way

steering is occurred in the reverse direction $m_2 \to m_1$ in Figure 2(b) where we used $n_{\text{th},1} = 5$ and $n_{\text{th},2} = 15$. Therefore, an appropriate choice of the temperatures T_1 and T_2 of the mechanical baths may provide a flexible and feasible experimental manner to manipulate the direction of one-way steering. To better explain the direction of one-way steering observed in Figure 2, we analyse the sign of the difference $\mathcal{E}_1 - \mathcal{E}_2$ where $\mathcal{E}_j = \frac{\hbar\omega_m}{2}(\langle\delta\tilde{q}^2_{m_j}\rangle + \langle\delta\tilde{p}^2_{m_j}\rangle)$ is the mean energy of the jth mechanical mode. In Figure 3 we plot $\mathcal{E}_1 - \mathcal{E}_2$, in units of $\hbar\omega_m/2$, under the same conditions as in Figure 2. As can be seen, the direction of one-way steering is strongly influenced by the sign of the difference $\mathcal{E}_1 - \mathcal{E}_2$. Indeed, in the situation where $\mathcal{E}_1 - \mathcal{E}_2$ remains positive, which corresponds to $n_{\text{th},1} = 15$ and $n_{\text{th},2} = 5$, one-way steering is occurred from $m_1 \to m_2$ in Figure 2(a). While for $n_{\text{th},1} = 5$ and $n_{\text{th},2} = 15$, $\mathcal{E}_1 - \mathcal{E}_2$ remains negative and one-way steering is occurred from $m_2 \to m_1$ in Figure 2(b). Physically this could be interpreted as follows: for a two-mode Gaussian state subject to Gaussian measurements, the mode having a higher fluctuation is more difficult to be steered by the other mode having a lower fluctuation.

Next, in Figure 4 we plot the steerabilities $\mathcal{G}^{m_1\to m_2}$ and $\mathcal{G}^{m_2\to m_1}$ versus Ω/γ using $n_{\text{th},1,2} = 15$ and two different values of the common effective optomechanical coupling $G_{1,2}/\omega_m \equiv G/\omega_m$, namely, $G/\omega_m = 0.25$ in Figure 4(a) and $G/\omega_m = 0.35$ in Figure 4(b). In contrary to the results depicted in Figure 2, Figure 4 shows, under the use of balanced thermal occupations and balanced effective optomechanical couplings, the occurrence of one-way steering only from $m_2 \to m_1$. Importantly, the increasing of G/ω_m from 0.25 to 0.35 enlarges drastically the range of Ω/γ corresponding to one-way steering. This indicates the advantage of the mediation of the optomechanical coupling in achieving one-way steering through a wide range of Ω/γ, which provides the asymmetric guaranteed key rate achievable within a practical 1SDI-QKD [29].

It is well known that real quantum systems are inevitably affected by their surrounding environments which leads to the degradation of quantum correlations via decoherence process. This is a challenging issue for creating and preserving quantum correlations in open systems which is of great importance for quantum information processing. In Figure 5, we study $\mathcal{G}^{m_1\to m_2}$ and $\mathcal{G}^{m_2\to m_1}$ under influence of the common mean thermal phonon number $n_{\text{th},1,2} = n_{\text{th}}$ and the normalized driving field strength Ω/γ using $G_1/\omega_m = 0.25$ and $G_2/\omega_m = 0.35$ in [Figures 5(a) and 5(b)], while $G_1/\omega_m = 0.35$ and $G_2/\omega_m = 0.25$ in [Figures 5(c) and 5(d)]. It is vividly shown that both steerabilities $\mathcal{G}^{m_1\to m_2}$ and $\mathcal{G}^{m_2\to m_1}$ are maximum close to $n_{\text{th}} = 0$, however with increasing n_{th}, they decrease gradually and eventually disappear.

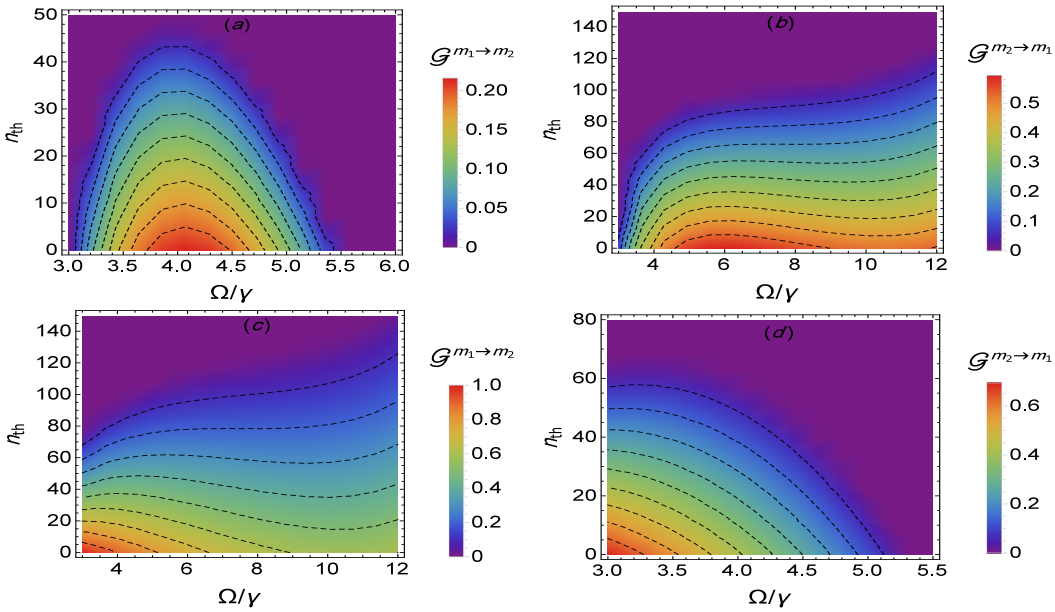

Figure 5: Density plot of the Gaussian steerabilities $\mathcal{G}^{m_1\to m_2}$ and $\mathcal{G}^{m_2\to m_1}$ versus the normalized driving field strength Ω/γ and the common mean thermal phonon number $n_{\text{th},1,2} = n_{\text{th}}$ using $\kappa = 2\pi \times 215$ kHz, $\gamma_m = 2\pi \times 140$ Hz, $\omega_m = 2\pi \times 947$ kHz, and $\mathcal{A} = 250$ MHz. For the effective optomechanical coupling strengths, we used $G_1/\omega_m = 0.25$ and $G_2/\omega_m = 0.35$ in [(a) and (b)], while $G_1/\omega_m = 0.35$ and $G_2/\omega_m = 0.25$ in [(c) and (d)]. In the appendix, we show that the chosen values of G_1, G_2, and Ω/γ fulfill the stability conditions derived using the Routh-Hurwitz criterion [62].

Interestingly, Figure 5 shows that $\mathcal{G}^{m_1\to m_2}$ and $\mathcal{G}^{m_2\to m_1}$ exhibit rather different trends against thermal noise that, not only reduces the degree of $\mathcal{G}^{m_1\to m_2}$ and $\mathcal{G}^{m_2\to m_1}$, but also it could play a constructive role in inducing one-way steering via a suitable choice of the ratio G_1/G_2. Indeed, in [Figures 5(a) and 5(b)] where $G_1/G_2 < 1$, $\mathcal{G}^{m_1\to m_2}$ vanishes entirely for $n_{\text{th}} > 45$, while $\mathcal{G}^{m_2\to m_1}$ still persists and it is significantly nonzero for thermal occupancy up to $n_{\text{th}} \approx 120$ meaning that the state $\varrho_{m_1m_2}$ is one-way steerable from $m_2 \to m_1$ for $45 \leqslant n_{\text{th}} \leqslant 120$. Whereas, [Figures 5(c) and 5(d)] show that for $G_1/G_2 > 1$, $\mathcal{G}^{m_2\to m_1}$ vanishes for $n_{\text{th}} > 60$, while $\mathcal{G}^{m_1\to m_2}$ is fairly robust against thermal noise up to $n_{\text{th}} \approx 145$ meaning that the state $\varrho_{m_1m_2}$ is one-way steerable from $m_1 \to m_2$

for $60 \leqslant n_{\rm th} \leqslant 145$. Then, one concludes that the direction of one-way steering between the two mechanical modes m_1 and m_2 can be manipulated with the temperatures of the mechanical baths and the optomechanical coupling strengths.

In Figure 6(a) we plot the difference $\mathcal{E}_1 - \mathcal{E}_2$ for the same conditions as in [Figures 5(a) and 5(b)], whereas in Figure 6(b) we plot $\mathcal{E}_1 - \mathcal{E}_2$ for the same conditions as in [Figures 5(c) and 5(d)]. We also remark that the direction of one-way steering depends on the sign of the difference $\mathcal{E}_1 - \mathcal{E}_2$, i.e., in Figure 6(a) where $\mathcal{E}_1 - \mathcal{E}_2 < 0$, one-way steering is occurred from $m_2 \to m_1$ in [Figures 5(a) and 5(b)], while in Figure 6(b) where $\mathcal{E}_1 - \mathcal{E}_2 > 0$, one-way steering is occurred from $m_1 \to m_2$ in [Figures 5(c) and 5(d)]. This is in concordance with the results obtained in Figures 2 and 3.

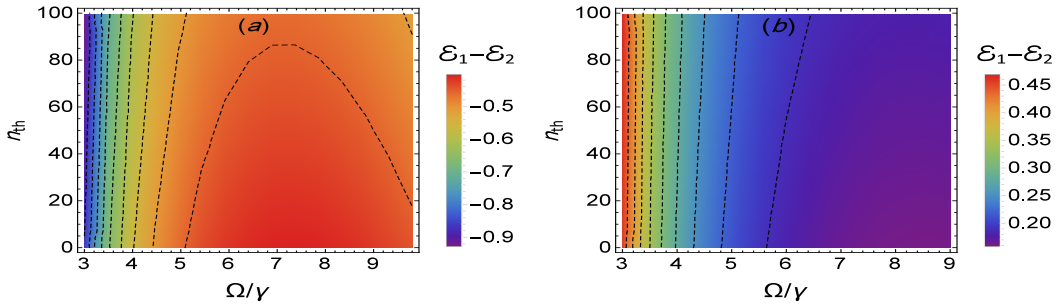

Figure 6: Plot of $\mathcal{E}_1 - \mathcal{E}_2$, in units of $\frac{1}{2}\hbar\omega_m$, versus Ω/γ and $n_{\rm th}$. The parameters in (a) and (b) are the same as in [Figures 5(a) and 5(b)] and [Figures 5(c) and 5(d)], respectively.

Since the security of 1SDI-QKD protocol depends crucially on the direction of steering, the presented scheme may be useful for such protocol, where two-way steering can be regarded as part of a legitimate step of the protocol [20], while one-way steering can be considered as an attack from an adversarial party [20]. On the other hand, the change in the direction of steering may change the role played by two persons during their communication employing 1SDI-QKD protocol, which is of great practical importance in the security of such protocol [20].

With the stability conditions given in Appendix A and experimentally accessible parameters [43, 44, 45, 46], macroscopic asymmetric Gaussian steering for two vibrating mirrors may be realized with the current state-of-the-art experimental apparatus. Furthermore, by exploiting the measurement strategy proposed in [31, 61], the covariance matrix (29) can be fully reconstructed using standard homodyne detection [63], which allows us to estimate numerically the steerabilities $\mathcal{G}^{m_1\to m_2}$ and $\mathcal{G}^{m_2\to m_1}$.

5 Conclusion

We have investigated a scheme for generating asymmetric steering between two non-interacting mechanical modes m_1 and m_2 by transferring quantum correlations from a correlated-emission laser through radiation pressure. The laser's gain medium consists of a set of nondegenerate three-level atoms in a cascade configuration. By applying the master equation for a two-mode laser, we derived the linearized quantum Langevin equations that describe the optomechanical coupling between modes m_1 and m_2 and the two cavity modes. These equations were then used to obtain the covariance matrix for modes m_1 and m_2 in the steady state. Using realistic experimental parameters, we demonstrated that both two-way and one-way steering can be observed by varying the strength of the external field driving the gain medium. Unlike most schemes that rely on optical losses to control the direction of one-way steering, our findings indicate that the direction of one-way steering can be adjusted on demand by modifying either the optomechanical coupling strengths or the temperatures of the mechanical baths, providing a flexible and practical approach for experimental implementation. Additionally, we revealed that the direction of one-way steering is influenced by mode fluctuations, with the mechanical mode exhibiting higher fluctuations dominating the directionality.

Our results demonstrate a viable method for manipulating the direction of one-way steering in a doubly resonant optomechanical cavity, which may have potential applications in one-way quantum information tasks, such as one-way quantum computation and communication.

Appendix A: Stability Analysis

We provide here the stability analysis via the Routh–Hurwitz criterion [62] to ensure the choice of parameters made during the study of the steerabilities $\mathcal{G}^{m_1\to m_2}$ and $\mathcal{G}^{m_2\to m_1}$. The Routh-Hurwitz criterion asserts that the system can reach a stable steady state when all real parts of the eigenvalues χ of the matrix $\mathcal{K}$ (24) are negative. The eigenvalues χ are given by the roots of the characteristic equation $\det(\mathcal{K} - \chi\mathbb{1}_8) = 0$ which can be reduced to $a_0\chi^8 + a_1\chi^7 + a_2\chi^6 + a_3\chi^5 + a_4\chi^4 + a_5\chi^3 + a_6\chi^2 + a_7\chi + a_8 = 0$, where the coefficients a_i are too cumbersome to be reported here.

In fact, the Routh-Hurwitz criterion constrains the coefficients $a_i (i = 0, .., 8)$, and then the system parameters, through the Hurwitz determinants obtained from the determinant

$$\Lambda_n = \begin{vmatrix} a_1 & a_3 & a_5 & \dots & 0 & 0 \\ a_0 & a_2 & a_4 & \dots & 0 & \vdots \\ 0 & a_1 & a_3 & \dots & 0 & \vdots \\ 0 & a_0 & a_2 & \ddots & a_n & \vdots \\ 0 & \dots & \dots & a_{n-3} & a_{n-1} & 0 \\ 0 & \dots & \dots & a_{n-4} & a_{n-2} & a_n \end{vmatrix}, \tag{31}$$

with $a_0 = 1$, $\Lambda_1 = a_1$, $\Lambda_2 = \begin{vmatrix} a_1 & a_3 \\ a_0 & a_2 \end{vmatrix}$, $\Lambda_3 = \begin{vmatrix} a_1 & a_3 & a_5 \\ a_0 & a_2 & a_4 \\ 0 & a_1 & a_3 \end{vmatrix}$, ..., $\Lambda_8 = \begin{vmatrix} a_1 & a_3 & a_5 & a_7 & 0 & 0 & 0 & 0 \\ a_0 & a_2 & a_4 & a_6 & a_8 & 0 & 0 & 0 \\ 0 & a_1 & a_3 & a_5 & a_7 & 0 & 0 & 0 \\ 0 & a_0 & a_2 & a_4 & a_6 & a_8 & 0 & 0 \\ 0 & 0 & a_1 & a_3 & a_5 & a_7 & 0 & 0 \\ 0 & 0 & a_0 & a_2 & a_4 & a_6 & a_8 & 0 \\ 0 & 0 & 0 & a_1 & a_3 & a_5 & a_7 & 0 \\ 0 & 0 & 0 & a_0 & a_2 & a_4 & a_6 & a_8 \end{vmatrix}$.

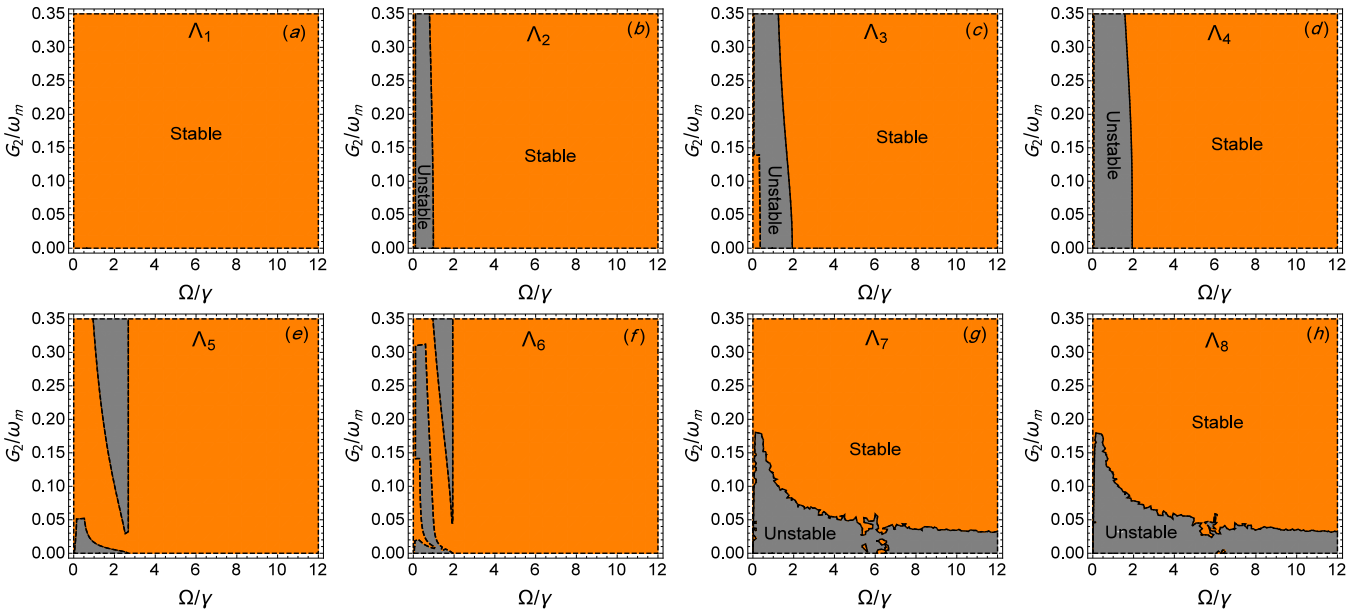

Figure 7: Plot of the Hurwitz determinants Λ_n for $n = 1, .., 8$ versus the Ω/γ and G_2/ω_m using $G_1/\omega_m = 0.25$, $\omega_m = 2\pi \times 947$ kHz, $\kappa = 2\pi \times 215$ kHz, $\gamma_m = 2\pi \times 140$, and $\mathcal{A} = 250$ MHz. The orange part is the stable area, while the gray one is the unstable area.

In Figure 7, we plot the determinants Λ_n for $n = 1, .., 8$ using $G_1/\omega_m = 0.25$, $0 \leqslant G_2/\omega_m \leqslant 0.35$, $0 \leqslant \Omega/\gamma \leqslant 12$, $\omega_m = 2\pi \times 947$ kHz, $\kappa = 2\pi \times 215$ kHz, $\gamma_m = 2\pi \times 140$ Hz, and $\mathcal{A} = 250$ MHz. As can be seen from in Figure 7(a), the determinant Λ_1 remains positive, then according to the Routh-Hurwitz criterion, the real parts of the eigenvalues of the matrix $\mathcal{K}$ (24) are all negative if and only if the sequence of the determinants Λ_n for $n = 2,..,$ 8 are all positive. For $0.2 \leqslant G_2/\omega_m \leqslant 0.35$ and $3 \leqslant \Omega/\gamma \leqslant 12$, we have $\Lambda_n > 0$ for $n = 1, .., 8$, meaning that the values of G_1/ω_m, G_2/ω_m, and Ω/γ, considered in our numerical simulations, guarantee the stability of our system.

Appendix B: Derivation of Equation (3)

In this Appendix, employing the procedure outlined in refs. [53, 55], we derive the master equation of the reduced density matrix $\rho_{o_1 o_2}$ for two-mode laser o_1 and o_2 generated when a single three-level atom makes transitions from $|\ell_1\rangle \rightarrow |\ell_2\rangle$ and $|\ell_2\rangle \rightarrow |\ell_3\rangle$, respectively [Figure 1(b)]. First, we adopt $\rho_{(\mathrm{sa},o_1 o_2)}(t, t_j)$ to represent the density matrix at time t for the modes o_1 and o_2 plus a single atom pumped into the cavity at an earlier time t_j. Then, the density matrix of the atomic system plus the modes o_1 and o_2 in the cavity at time t writes $\rho_{(\mathrm{sa},o_1 o_2)}(t) = r_0 \sum_j \rho_{(\mathrm{sa},o_1 o_2)}(t, t_j)\Delta t$, where $r_0 \Delta t$ yields the number of atoms injected into the cavity within a brief time interval Δt. The atoms are injected into the cavity at a rate r_0 and removed after a time τ, supposed, longer than the spontaneous emission time [36]. During this time interval τ, a single atom resonantly interacts with the cavity modes of frequencies ν_1 and ν_2.

When $\Delta t \to 0$, the summation can be approximated by integration, i.e.,

$$\rho_{(\mathrm{sa},o_1o_2)}(t) = r_0 \int_{t-\tau}^{t} \rho_{(\mathrm{sa},o_1o_2)}(t,t')dt' \text{ with } t-\tau \leqslant t' \leqslant t. \tag{32}$$

Now differentiating both sides of Equation (32), we get $\frac{d\rho_{(\mathrm{sa},o_1o_2)}(t)}{dt} = r_0 \frac{d}{dt}\int_{t-\tau}^{t} \rho_{(\mathrm{sa},o_1o_2)}(t,t')dt'$, which can be expanded by means of the Leibnitz rule as

$$\frac{d\rho_{(\mathrm{sa},o_1o_2)}(t)}{dt} = r_0 \left[\rho_{(\mathrm{sa},o_1o_2)}(t,t) - \rho_{(\mathrm{sa},o_1o_2)}(t,t-\tau)\right] + r_0 \int_{t-\tau}^{t} \frac{\partial \rho_{(\mathrm{sa},o_1o_2)}(t,t')}{\partial t} dt'. \tag{33}$$

In the Markov approximation [65] where the atomic and laser modes states are assumed to be uncorrelated at the instant t in which the atoms are injected in the cavity, we have $\rho_{(\mathrm{sa},o_1o_2)}(t,t) = \rho_{o_1o_2}(t)\rho_{\mathrm{sa}}(0)$. Besides, we suppose that all the three-level atoms to be initially injected into the cavity in the lower energy level $|\ell_3\rangle$. Then, the corresponding initial density operator reads $\rho_{\mathrm{sa}}(0) = |\ell_3\rangle\langle\ell_3|$. Furthermore, assuming that the atomic and laser modes states are uncorrelated just after the atoms left the cavity, which allows us to write $\rho_{(\mathrm{sa},o_1o_2)}(t,t-\tau) = \rho_{o_1o_2}(t)\rho_{\mathrm{sa}}(t-\tau)$, therefore Equation (33) yields

$$\frac{d\rho_{(\mathrm{sa},o_1o_2)}(t)}{dt} = r_0 \left[\rho_{\mathrm{sa}}(0) - \rho_{\mathrm{sa}}(t-\tau)\right] \rho_{o_1o_2}(t) + r_0 \int_{t-\tau}^{t} \frac{\partial \rho_{(\mathrm{sa},o_1o_2)}(t,t')}{\partial t} dt', \tag{34}$$

where $\rho_{\mathrm{sa}}(t-\tau)$ is the density operator for a single atom pumped at $t-\tau$. Henceforth, we use $\rho_{o_1o_2}(t) \equiv \rho$ for simplicity of notation.

Obviously, we have $\frac{\partial}{\partial t}\rho_{(\mathrm{sa},o_1o_2)}(t) = \frac{-\mathrm{i}}{\hbar}[\mathcal{H}_{af}^{int} + \mathcal{H}_{ac}^{int}, \rho_{(\mathrm{sa},o_1o_2)}(t)]$ which together with Equations (32) and (34) leads to

$$\frac{d\rho_{(\mathrm{sa},o_1o_2)}(t)}{dt} = r_0 \left[\rho_{\mathrm{sa}}(0) - \rho_{\mathrm{sa}}(t-\tau)\right] \rho - \frac{\mathrm{i}}{\hbar}[\mathcal{H}_{af}^{int} + \mathcal{H}_{ac}^{int}, \rho_{(\mathrm{sa},o_1o_2)}(t)]. \tag{35}$$

Next, taking into account the damping of the two-mode laser o_1 and o_2 by the vacuum reservoir, and tracing both sides of Equation (35) over the atomic variables, we get

$$\frac{d\rho}{dt} = \frac{-\mathrm{i}}{\hbar}\mathrm{Tr}_{\mathrm{sa}}[\mathcal{H}_{af}^{int} + \mathcal{H}_{ac}^{int}, \rho_{(\mathrm{sa},o_1o_2)}(t)] + \sum_{j=1,2} \kappa_j \mathcal{L}\left[c_j\right]\rho, \tag{36}$$

where we used $\mathrm{Tr}_{\mathrm{sa}}\rho_{\mathrm{sa}}(0) = \mathrm{Tr}_{\mathrm{sa}}\rho_{\mathrm{sa}}(t-\tau) = 1$ and $\mathrm{Tr}_{\mathrm{sa}}\rho_{(\mathrm{sa},o_1o_2)}(t) = \rho$, with $\mathcal{L}\left[c_j\right]\rho = 2c_j\rho c_j^{\dagger} - \{c_j^{\dagger}c_j, \rho\}_+$ being the Lindblad damping term [54]. Replacing $\mathcal{H}_{af}^{int}$ and $\mathcal{H}_{ac}^{int}$ by their expressions in Equation (36) and tracing out the atomic variables, we find

$$\begin{aligned} \frac{d\rho}{dt} &= \varsigma(\rho_{12}c_1^{\dagger} - c_1^{\dagger}\rho_{12} + \rho_{23}c_2^{\dagger} - c_2^{\dagger}\rho_{23} + c_1\rho_{21} - \rho_{21}c_1 + c_2\rho_{32} - \rho_{32}c_2) + \\ &\quad \sum_{j=1,2} \kappa_j \mathcal{L}\left[c_j\right]\rho, \end{aligned} \tag{37}$$

where we used the notation $\rho_{mn} = \langle \ell_m|\rho_{(\mathrm{sa},o_1o_2)}|\ell_n\rangle$ for $m,n = 1,2,3$.

Now, we determine the density operators ρ_{12} and ρ_{23} involved in Equation (37). For this, we multiply Equation (35) on the left by $\langle \ell_m|$, and on the right by $|\ell_n\rangle$, furthermore we assume that the atoms decay to energy levels other than $|\ell_1\rangle$, $|\ell_2\rangle$ or $|\ell_3\rangle$ when they leave the cavity, i.e., $\langle \ell_m \left|\rho_{\mathrm{sa}}(t-\tau)\right| \ell_n\rangle = 0$. Then, we get

$$\frac{d\rho_{mn}}{dt} = r_0\langle \ell_m \left|\rho_{\mathrm{sa}}(0)\right| \ell_n\rangle\rho - \frac{\mathrm{i}}{\hbar}\langle \ell_m|[\mathcal{H}_{af}^{int} + \mathcal{H}_{ac}^{int}, \rho_{(\mathrm{sa},o_1o_2)}]|\ell_n\rangle - \gamma_{mn}\rho_{mn}, \tag{38}$$

where the coefficients γ_{mn} are added to account for the spontaneous emission and dephasing processes [36].

Hence, using the fact that $\rho_{\mathrm{sa}}(0) = |\ell_3\rangle\langle\ell_3|$ and the expressions of $\mathcal{H}_{af}^{int}$ and $\mathcal{H}_{ac}^{int}$ together with Equation (38),

we obtain

$$\frac{d\rho_{11}}{dt} = \varsigma(c_1\rho_{21} + \rho_{12}c_1^\dagger) - \frac{\Omega}{2}(\rho_{13} + \rho_{31}) - \gamma_1\rho_{11}, \tag{39}$$

$$\frac{d\rho_{22}}{dt} = -\varsigma(c_1^\dagger\rho_{12} + \rho_{21}c_1 - c_2\rho_{32} - \rho_{23}c_2^\dagger) - \gamma_2\rho_{22}, \tag{40}$$

$$\frac{d\rho_{33}}{dt} = r_0\rho - \varsigma(c_2^\dagger\rho_{23} + \rho_{32}c_2) + \frac{\Omega}{2}(\rho_{13} + \rho_{31}) - \gamma_3\rho_{33}, \tag{41}$$

$$\frac{d\rho_{13}}{dt} = \varsigma(c_1\rho_{23} - \rho_{12}c_2) - \frac{\Omega}{2}(\rho_{33} - \rho_{11}) - \gamma_{13}\rho_{13}, \tag{42}$$

$$\frac{d\rho_{12}}{dt} = \varsigma(c_1\rho_{22} - \rho_{11}c_1 + \rho_{13}c_2^\dagger) - \frac{\Omega}{2}\rho_{32} - \gamma_{12}\rho_{12}, \tag{43}$$

$$\frac{d\rho_{32}}{dt} = -\varsigma(\rho_{31}c_1 - \rho_{33}c_2^\dagger + c_2^\dagger\rho_{22}) + \frac{\Omega}{2}\rho_{12} - \gamma_{23}\rho_{32}, \tag{44}$$

where γ_j $(j = 1, 2, 3)$ refers to the jth atomic-level spontaneous emission decay rate, γ_{13} represents the two-photon dephasing rate, whereas γ_{12} and γ_{23} denote the single-photon dephasing rates [53]. From now on, we take for simplicity $\gamma_1 = \gamma_2 = \gamma_3 = \gamma_{12} = \gamma_{13} = \gamma_{23} \equiv \gamma$.

Subsequently, in the good cavity limit where $\kappa_j \ll \gamma_j$, the atomic states reach the stationary regime much faster than the laser modes [36]. Then we can adiabatically eliminate the dynamics of the atoms by setting the time derivatives in Equations [(39)-(42)] to zero. On the other hand, applying the linear approximation [36, 53], one can eliminate the terms proportional to ς in the same equations. Thusly

$$-\frac{\Omega}{2}(\rho_{13} + \rho_{31}) - \gamma\rho_{11} = 0, \tag{45}$$

$$\rho_{22} = 0, \tag{46}$$

$$r_0\rho + \frac{\Omega}{2}(\rho_{13} + \rho_{31}) - \gamma\rho_{33} = 0, \tag{47}$$

$$-\frac{\Omega}{2}(\rho_{33} - \rho_{11}) - \gamma\rho_{13} = 0. \tag{48}$$

From Equation (48), we could simply verify that $\rho_{13} = \rho_{31}$, and in view of Equations (45), (47), and (48), we obtain

$$\rho_{11} = \frac{r_0\rho\Omega^2}{2\gamma(\gamma^2 + \Omega^2)}, \tag{49}$$

$$\rho_{33} = \frac{r_0\rho\left(2\gamma^2 + \Omega^2\right)}{2\gamma(\gamma^2 + \Omega^2)}, \tag{50}$$

$$\rho_{13} = -\frac{r_0\rho\Omega}{2(\gamma^2 + \Omega^2)}. \tag{51}$$

Next, injecting Equations (46), (49), (50) and (51) in Equations (43) and (44), and performing the adiabatic elimination once again, we get

$$\rho_{12} = \frac{-\varsigma r_0\rho}{(4\gamma^2 + \Omega^2)(\gamma^2 + \Omega^2)}\left(3\Omega^2 c_1 + \frac{\Omega\left(4\gamma^2 + \Omega^2\right)}{\gamma}c_2^\dagger\right), \tag{52}$$

$$\rho_{32} = \frac{\varsigma r_0\rho}{(4\gamma^2 + \Omega^2)(\gamma^2 + \Omega^2)}\left(\frac{-\Omega\left(-2\gamma^2 + \Omega^2\right)}{\gamma}c_1 + \left(4\gamma^2 + \Omega^2\right)c_2^\dagger\right). \tag{53}$$

Finally, inserting Equations (52) and (53) into Equation (37), we arrive at Equation (3).

Appendix C: Derivation of Equations (6) and (7)

In terms of the master equation (3) and the formula $\frac{d\langle\mathcal{O}\rangle}{dt} = \mathrm{Tr}\left(\frac{d\rho}{dt}\mathcal{O}\right)$, we have

$$
\begin{aligned}
\frac{d\langle c_1\rangle}{dt} &= \Xi_{11}\mathrm{Tr}\left(2c_1^\dagger\rho c_1c_1 - c_1c_1^\dagger\rho c_1 - \rho c_1c_1^\dagger c_1\right) + \Xi_{22}\mathrm{Tr}\left(2c_2\rho c_2^\dagger c_1 - c_2^\dagger c_2\rho c_1 - \rho c_2^\dagger c_2c_1\right)\\
&-\Xi_{12}\mathrm{Tr}\left(c_1c_2\rho c_1 - c_2\rho c_1c_1\right) - \Xi_{21}\mathrm{Tr}\left(\rho c_1c_2c_1 - c_2\rho c_1c_1\right)\\
&-\Xi_{12}\mathrm{Tr}\left(\rho c_1^\dagger c_2^\dagger c_1 - c_1^\dagger\rho c_2^\dagger c_1\right) - \Xi_{21}\mathrm{Tr}\left(c_1^\dagger c_2^\dagger\rho c_1 - c_1^\dagger\rho c_2^\dagger c_1\right)\\
&+\kappa_1\mathrm{Tr}\left(2c_1\rho c_1^\dagger c_1 - c_1^\dagger c_1\rho c_1 - \rho c_1^\dagger c_1c_1\right) + \kappa_2\mathrm{Tr}\left(2c_2\rho c_2^\dagger c_1 - c_2^\dagger c_2\rho c_1 - \rho c_2^\dagger c_2c_1\right), \qquad (54)
\end{aligned}
$$

where we employed the linearity property of the trace operator.

Now, we calculate the eight traces, that appear in Equation (54), using the cyclic property of the trace operator, and the facts that $[c_k, c_{k'}] = \left[c_k^\dagger, c_{k'}^\dagger\right] = 0$ and $\left[c_k, c_{k'}^\dagger\right] = \delta_{kk'}$ for $k,\ k' = 1, 2$, i.e.,

$$
\begin{aligned}
\mathcal{T}_1 &= \Xi_{11}\mathrm{Tr}\left(2c_1^\dagger\rho c_1c_1 - c_1c_1^\dagger\rho c_1 - \rho c_1c_1^\dagger c_1\right),\\
&= \Xi_{11}\mathrm{Tr}\left(2\rho c_1c_1c_1^\dagger - \rho c_1c_1c_1^\dagger - \rho c_1c_1^\dagger c_1\right),\\
&= \Xi_{11}\mathrm{Tr}\left(\rho c_1c_1c_1^\dagger - \rho c_1c_1^\dagger c_1\right) = \Xi_{11}\mathrm{Tr}\left(\rho c_1\left[c_1c_1^\dagger - c_1^\dagger c_1\right]\right),\\
&= \Xi_{11}\mathrm{Tr}\left(\rho c_1\right) = \Xi_{11}\langle c_1\rangle. \qquad (55)
\end{aligned}
$$

$$
\begin{aligned}
\mathcal{T}_2 &= \Xi_{22}\mathrm{Tr}\left(2c_2\rho c_2^\dagger c_1 - c_2^\dagger c_2\rho c_1 - \rho c_2^\dagger c_2c_1\right),\\
&= \Xi_{22}\mathrm{Tr}\left(2\rho c_2^\dagger c_1c_2 - \rho c_1c_2^\dagger c_2 - \rho c_2^\dagger c_2c_1\right),\\
&= \Xi_{22}\mathrm{Tr}\left(2\rho c_2^\dagger c_2c_1 - \rho c_2^\dagger c_2c_1 - \rho c_2^\dagger c_2c_1\right) = 0. \qquad (56)
\end{aligned}
$$

$$
\begin{aligned}
\mathcal{T}_3 &= -\Xi_{12}\mathrm{Tr}\left(c_1c_2\rho c_1 - c_2\rho c_1c_1\right),\\
&= -\Xi_{12}\mathrm{Tr}\left(\rho c_1c_1c_2 - \rho c_1c_1c_2\right) = 0. \qquad (57)
\end{aligned}
$$

$$
\begin{aligned}
\mathcal{T}_4 &= -\Xi_{21}\mathrm{Tr}\left(\rho c_1c_2c_1 - c_2\rho c_1c_1\right),\\
&= -\Xi_{21}\mathrm{Tr}\left(\rho c_1c_2c_1 - \rho c_1c_1c_2\right),\\
&= -\Xi_{21}\mathrm{Tr}\left(\rho c_1c_1c_2 - \rho c_1c_1c_2\right) = 0. \qquad (58)
\end{aligned}
$$

$$
\begin{aligned}
\mathcal{T}_5 &= -\Xi_{12}\mathrm{Tr}\left(\rho c_1^\dagger c_2^\dagger c_1 - c_1^\dagger\rho c_2^\dagger c_1\right),\\
&= -\Xi_{12}\mathrm{Tr}\left(\rho c_1^\dagger c_2^\dagger c_1 - \rho c_2^\dagger c_1c_1^\dagger\right),\\
&= -\Xi_{12}\mathrm{Tr}\left(\rho c_2^\dagger\left[c_1^\dagger c_1 - c_1c_1^\dagger\right]\right) = \Xi_{12}\mathrm{Tr}\left(\rho c_2^\dagger\right),\\
&= \Xi_{12}\langle c_2^\dagger\rangle. \qquad (59)
\end{aligned}
$$

$$
\begin{aligned}
\mathcal{T}_6 &= -\Xi_{21}\mathrm{Tr}\left(c_1^\dagger c_2^\dagger\rho c_1 - c_1^\dagger\rho c_2^\dagger c_1\right),\\
&= -\Xi_{21}\mathrm{Tr}\left(\rho c_1c_1^\dagger c_2^\dagger - \rho c_2^\dagger c_1c_1^\dagger\right) = 0. \qquad (60)
\end{aligned}
$$

$$
\begin{aligned}
\mathcal{T}_7 &= \kappa_1\mathrm{Tr}\left(2c_1\rho c_1^\dagger c_1 - c_1^\dagger c_1\rho c_1 - \rho c_1^\dagger c_1c_1\right),\\
&= \kappa_1\mathrm{Tr}\left(2\rho c_1^\dagger c_1c_1 - \rho c_1c_1^\dagger c_1 - \rho c_1^\dagger c_1c_1\right),\\
&= \kappa_1\mathrm{Tr}\left(\rho c_1^\dagger c_1c_1 - \rho c_1c_1^\dagger c_1\right) = \kappa_1\mathrm{Tr}\left(\rho\left[c_1^\dagger c_1 - c_1c_1^\dagger\right]c_1\right),\\
&= -\kappa_1\mathrm{Tr}\left(\rho c_1\right) = -\kappa_1\langle c_1\rangle. \qquad (61)
\end{aligned}
$$

$$
\begin{aligned}
\mathcal{T}_8 &= \kappa_2 \mathrm{Tr}\left(2c_2\rho c_2^\dagger c_1 - c_2^\dagger c_2 \rho c_1 - \rho c_2^\dagger c_2 c_1\right), \\
&= \kappa_2 \mathrm{Tr}\left(2\rho c_2^\dagger c_1 c_2 - \rho c_1 c_2^\dagger c_2 - \rho c_2^\dagger c_2 c_1\right), \\
&= \kappa_2 \mathrm{Tr}\left(2\rho c_2^\dagger c_2 c_1 - \rho c_2^\dagger c_2 c_1 - \rho c_2^\dagger c_2 c_1\right) = 0. \qquad (62)
\end{aligned}
$$

On the basis of Equations [(55)-(62)], we get

$$
\begin{aligned}
\frac{d\langle c_1\rangle}{dt} &= \mathcal{T}_1 + \mathcal{T}_2 + \mathcal{T}_3 + \mathcal{T}_4 + \mathcal{T}_5 + \mathcal{T}_6 + \mathcal{T}_7 + \mathcal{T}_8, \\
&= -\kappa_1\langle c_1\rangle + \Xi_{11}\langle c_1\rangle + \Xi_{12}\langle c_2^\dagger\rangle. \qquad (63)
\end{aligned}
$$

Therefore, Equation (6) can be now obtained by removing the bracket from Equation (63), and adding the noise operator $\digamma_1$ with zero mean value, i.e., $\langle \digamma_1 \rangle$. Finally, following the same approach presented in this Appendix, Equation (7) can be established.

Acknowledgements

The authors gratefully acknowledge computational resources from the 2MS team faculty of sciences Meknes. The authors acknowledge the PPR2 project: (MESRSI-CNRST).

Conflict of Interest

The authors declare no conflict of interest.

Data Availability Statement

Research data are not shared.

References

[1] A. Einstein, B. Podolsky, N. Rosen, *Phys. Rev.* **1935**, 47, 777.

[2] E. Schrödinger, *Math. Proc. Cambridge Philos. Soc.* **1935**, 31, 555.

[3] E. Schrödinger, *Math. Proc. Cambridge Philos. Soc.* **1936**, 32, 446.

[4] H. M. Wiseman, S. J. Jones, A. C. Doherty, *Phys. Rev. Lett.* **2007**, 98, 140402.

[5] R. Uola, A. C. S. Costa, H. C. Nguyen, O. Gühne, *Rev. Mod. Phys.* **2020**, 92, 015001.

[6] R. Horodecki, P. Horodecki, M. Horodecki, K. Horodecki, *Rev. Mod. Phys.* **2009**, 81, 865.

[7] N. Brunner, D. Cavalcanti, S. Pironio, V. Scarani, S. Wehner, *Rev. Mod. Phys.* **2014**, 86, 419.

[8] O. Gühne, E. Haapasalo, T. Kraft, J. -P. Pellonpää, R. Uola, *Rev. Mod. Phys.* **2023**, 95, 011003.

[9] J. Bowles, T. Vértesi, M. T. Quintino, N. Brunner, *Phys. Rev. Lett.* **2014**, 112, 200402.

[10] J. E. Qars, M. Daoud, R. A. Laamara, *Phys. Rev. A* **2018**, 98, 042115.

[11] J. E. Qars, *Ann. Phys. (Berlin)* **2022**, 534(6), 2100386.

[12] Y. -H. Lin, Y. -Q. Lin, R. -C. Yang, H. -Y. Liu, *Adv. Quantum Tech.* **2024**, 7, 2400180.

[13] Q. -M. Wan, Y. -H. Lin, Y. -Q. Lin, L. -J. Cong, R. -C. Yang, H. -Y. Liu, *Ann. Phys. Berlin* **2024**, 536, 2300484.

[14] J. Wang, H. Cao, J. Jing, H. Fan, *Phys. Rev. D* **2016**, 93, 125011.

[15] K. Sun, J. -S. Xu, X. -J. Ye, Y. -C. Wu, J. -L. Chen, C. -F. Li, G. -C. Guo, *Phys. Rev. Lett.* **2014**, 113, 140402.

[16] S. Wollmann, N. Walk, A. J. Bennet, H. M. Wiseman, G. J. Pryde, *Phys. Rev. Lett.* **2016**, 116, 160403.

[17] S. Wollmann, R. Uola, A. C. S. Costa, *Phys. Rev. Lett.* **2020**, 125, 020404.

[18] S. Designolle, V. Srivastav, R. Uola, N. H. Valencia, W. McCutcheon, M Malik, N. Brunner, *Phys. Rev. Lett.* **2021**, 126, 200404.

[19] K. Sun, X.-J. Ye, J.-S. Xu, X.-Y. Xu, J.-S. Tang, Y.-C.Wu, J.-L. Chen, C.-F. Li, G.-C. Guo, *Phys. Rev. Lett.* **2016**, 116, 160404.

[20] C. Branciard, E. G. Cavalcanti, S. P. Walborn, V. Scarani, H. M. Wiseman, *Phys. Rev. A* **2012**, 85, 010301.

[21] S. Armstrong, M. Wang, R. Y. Teh, Q. Gong, Q. He, J. Janousek, H. A. Bachor, M. D. Reid, P. K. Lam, *Nat. Phys.* **2015**, 11, 167.

[22] C. M. Li, K. Chen, Y. N. Chen, Q. Zhang, Y. A. Chen, J. W. Pan, *Phys. Rev. Lett.* **2015**, 115, 010402.

[23] Q. Y. He, L. Rosales-Zárate, G. Adesso, M. D. Reid, *Phys. Rev. Lett.* **2015**, 115, 180502.

[24] M. Piani, J. Watrous, *Phys. Rev. Lett.* **2015**, 114, 060404.

[25] M. D. Reid, *Phys. Rev. A* **1989**, 40, 913.

[26] E. G. Cavalcanti, S. J. Jones, H. M. Wiseman, M. D. Reid, *Phys. Rev. A* **2009**, 80, 032112.

[27] E. G. Cavalcanti, M. J. W. Hall, H. M. Wiseman, *Phys. Rev. A* **2013**, 87, 032306.

[28] P. Skrzypczyk, M. Navascués, D. Cavalcanti, *Phys. Rev. Lett.* **2014**, 112, 180404.

[29] I. Kogias, A. R. Lee, S. Ragy, G. Adesso, *Phys. Rev. Lett.* **2015**, 114, 060403.

[30] M. Aspelmeyer, T. J. Kippenberg, F. Marquardt, *Rev. Mod. Phys.* **2014**, 86, 1391.

[31] T. A. Palomaki, J. D. Teufel, R. W. Simmonds, K. W. Lehnert, *Science* **2013**, 342, 710.

[32] T. P. Purdy, P. -L. Yu, R. W. Peterson, N. S. Kampel, C. A. Regal, *Phys. Rev. X* **2013**, 3, 031012.

[33] E. A. Sete, H. Eleuch, *J. Opt. Soc. Am. B* **2015**, 32, 971.

[34] C. Sommer, C. Genes, *Phys. Rev. Lett.* **2019**, 123, 203605.

[35] R. Ghobadi, S. Kumar, B. Pepper, D. Bouwmeester, A. I. Lvovsky, C. Simon, *Phys. Lett. Rev.* **2014**, 112, 080503.

[36] M. O. Scully, M. S. Zubairy, *Quantum Optics*, Cambridge University Press, Cambridge, **1997**.

[37] M. O. Scully, K. Wodkiewicz, M. S. Zubairy, J. Bergou, N. Lu, J. Meyer ter Vehn, *Phys. Rev. Lett.* **1988**, 60, 1832.

[38] H. Xiong, M. O. Scully, M. S. Zubairy, *Phys. Rev. Lett.* **2005**, 94, 023601.

[39] N. A. Ansari, *Phys. Rev. A* **1993**, 48, 4686.

[40] L. Zhou, Y. Han, J. Jing, W. Zhang, *Phys. Rev. A* **2011**, 83, 052117.

[41] W. Ge, M. Al-Amri, H. Nha, M. S. Zubairy, *Phys. Rev. A* **2013**, 88, 022338.

[42] M. Bekele, T. Yirgashewa, S. Tesfa, *Phys. Rev. A* **2023**, 107, 012417.

[43] S. Gröblacher, K. Hammerer, M. R. Vanner, M. Aspelmeyer, *Nature (London)* **2009**, 460, 724.

[44] O. Arcizet, P. -F. Cohadon, T. Briant, M. Pinard, A. Heidmann, *Nature (London)* **2006**, 444, 71.

[45] J. McKeever, A. Boca, A. D. Boozer, R. Miller, J. R. Buck, A. Kuzmich, H. J. Kimble, *Science* **2004**, 303, 1992.

[46] B. Weber, H. P. Specht, T. Müller, J. Bochmann, M. Mücke, D. L. Moehring, G. Rempe, *Phys. Rev. Lett.* **2009**, 102, 030501.

[47] C. -G. Liao, H. Xie, R. -X. Chen, M. -Y. Ye, X. -M. Lin, *Phys. Rev. A* **2020**, 101, 032120.

[48] H. Tan, W. Deng, Q. Wu, G. Li, *Phys. Rev. A* **2017**, 95, 053842.

[49] H. Tan, X. Zhang, G. Li, *Phys. Rev. A* **2015**, 91, 032121.

[50] Z. -B. Yang, X. -D. Liu, X. -Y. Yin, Y. Ming, H. -Y. Liu, R. -C. Yang, *Phy. Rev. Appl.* **2021**, 15, 024042.

[51] S. -X. Wu, C. -H. Bai, G. Li, C. -S. Yu, T. Zhang, *Opt. Express* **2024**, 32, 260.

[52] H. Tan, W. Deng, L. Sun, *Phys. Rev. A* **2019**, 99, 043834.

[53] M. H. Louisell, *Quantum Statistical Properties of Radiation*, Wiley, New York, **1973**.

[54] D. F. Walls, G. J. Milburn, *Quantum Optics*, Springer-Verlag, Berlin, **1994**.

[55] M. Sargent III, M. O. Scully, W. E. Lamb, Jr., *Laser Physics*, Addison-Wesley, Reading, **1974**.

[56] M. O. Scully, *Phys. Rev. Lett.* **1985**, 55, 2802.

[57] Sh. Barzanjeh, D. Vitali, P. Tombesi, G. J. Milburn, *Phys. Rev. A* **2011**, 84, 042342.

[58] C. Genes, A. Mari, D. Vitali, P. Tombesi, *Adv. At. Mol. Opt. Phys.* **2009**, 57, 33.

[59] R. Benguria, M. Kac, *Phys. Rev. Lett*, **1981**, 46, 1.

[60] Y. Wang, Z. -Y. Hao, J. -K. Li, Z. -H. Liu, K. Sun, J. -S. Xu, C. -F. Li, G. -C. Guo, *Phys. Rev. Lett.* **2023**, 130, 200202.

[61] D. Vitali, S. Gigan, A. Ferreira, H. R. Böhm, P. Tombesi, A. Guerreiro, V. Vedral, A. Zeilinger, M. Aspelmeyer, *Phys. Rev. Lett.* **2007**, 98, 030405.

[62] E. X. DeJesus, C. Kaufman, *Phys. Rev. A* **1987**, 35, 5288.

[63] V. D'Auria, S. Fornaro, A. Porzio, S. Solimeno, S. Olivares, M. G. A. Paris, *Phys. Rev. Lett.* **2009**, 102, 020502.

[64] J. Guo, R. Norte, S. Gröblacher, *Phys. Rev. Lett.* **2019**, 123, 223602.

[65] C. W. Gardiner, P. Zoller, *Quantum Noise*, Springer, NewYork, **1999**.